



OPEN ACCESS

# Born With Bristles: New Insights on the Kölliker's Organs of Octopus Skin

**Edited by:**

Rachel Collin,  
Smithsonian Tropical Research  
Institute (SI), United States

**Reviewed by:**

Carsten Lueter,  
Museum of Natural History Berlin  
(MfN), Germany  
Kevin Kocot,  
University of Alabama, United States  
Janice Voltzow,  
University of Scranton, United States  
Louise Page,  
University of Victoria, Canada

**\*Correspondence:**

Roger Villanueva  
roger@icm.csic.es

**†ORCID:**

Roger Villanueva  
[orcid.org/0000-0001-8122-3449](https://orcid.org/0000-0001-8122-3449)  
Montserrat Coll-Lladó  
[orcid.org/0000-0003-0169-4107](https://orcid.org/0000-0003-0169-4107)  
Fernando Á. Fernández-Álvarez  
[orcid.org/0000-0002-8679-7377](https://orcid.org/0000-0002-8679-7377)  
Laure Bonnaud-Ponticelli  
[orcid.org/0000-0001-7510-5032](https://orcid.org/0000-0001-7510-5032)  
Sergio A. Carrasco  
[orcid.org/0000-0002-8179-4222](https://orcid.org/0000-0002-8179-4222)  
Oscar Escolar  
[orcid.org/0000-0002-1785-0138](https://orcid.org/0000-0002-1785-0138)  
Ian G. Gleadall  
[orcid.org/0000-0002-5157-5117](https://orcid.org/0000-0002-5157-5117)  
Jaruwat Nabhitabhata  
[orcid.org/0000-0002-6357-9959](https://orcid.org/0000-0002-6357-9959)  
Nicolás Ortiz  
[orcid.org/0000-0002-9581-8504](https://orcid.org/0000-0002-9581-8504)  
Carlos Rosas  
[orcid.org/0000-0002-1301-7368](https://orcid.org/0000-0002-1301-7368)  
Pilar Sánchez  
[orcid.org/0000-0002-3776-7358](https://orcid.org/0000-0002-3776-7358)  
Janet R. Voight  
[orcid.org/0000-0002-7800-2327](https://orcid.org/0000-0002-7800-2327)  
Jim Swoger  
[orcid.org/0000-0003-3805-0073](https://orcid.org/0000-0003-3805-0073)

**Specialty section:**

This article was submitted to  
Marine Biology,  
a section of the journal  
Frontiers in Marine Science

**Received:** 23 December 2020

**Accepted:** 19 March 2021

**Published:** 10 May 2021

Roger Villanueva<sup>1\*</sup>, Montserrat Coll-Lladó<sup>2†</sup>, Laure Bonnaud-Ponticelli<sup>3†</sup>, Sergio A. Carrasco<sup>4†</sup>, Oscar Escolar<sup>1†</sup>, Fernando Á. Fernández-Álvarez<sup>1,5†</sup>, Ian G. Gleadall<sup>6,7†</sup>, Jaruwat Nabhitabhata<sup>8†</sup>, Nicolás Ortiz<sup>9†</sup>, Carlos Rosas<sup>10†</sup>, Pilar Sánchez<sup>1†</sup>, Janet R. Voight<sup>11†</sup> and Jim Swoger<sup>2†</sup>

<sup>1</sup> Institut de Ciències del Mar, ICM-CSIC, Barcelona, Spain, <sup>2</sup> European Molecular Biology Laboratory, Barcelona, Spain, <sup>3</sup> Laboratory BOREA UMR MNHN, CNRS 8067, SU, IRD207, Paris, France, <sup>4</sup> Millennium Nucleus for Ecology and Sustainable Management of Oceanic Islands, Departamento de Biología Marina, Facultad de Ciencias del Mar, Universidad Católica del Norte, Coquimbo, Chile, <sup>5</sup> Ryan Institute and School of Natural Sciences, National University of Ireland, Galway, Ireland, <sup>6</sup> Graduate School of Agricultural Science, Tohoku University, Sendai, Japan, <sup>7</sup> Okinawa Institute of Science and Technology, Okinawa, Japan, <sup>8</sup> Excellence Centre for Biodiversity of Peninsular Thailand (CBIPT), Faculty of Science, Prince of Songkla University, Hatyai, Thailand, <sup>9</sup> Laboratory of Cephalopods, Instituto de Biología de Organismos Marinos (IBIOMAR), CCT CONICET-CENPAT, Puerto Madryn, Argentina, <sup>10</sup> Unidad Multidisciplinaria de Docencia e Investigación, Facultad de Ciencias, Universidad Nacional Autónoma de México, Mérida, Mexico, <sup>11</sup> Negaunee Integrative Research Center, Field Museum of Natural History, Chicago, IL, United States

The entire skin surface of octopus embryos, hatchlings and juveniles bears scattered tufts of tiny chitinous setae within small pockets, from which they can be everted and retracted. Known as Kölliker's organs (KO), they disappear before the subadult stage. The function of these structures during the early life of the octopus is unknown, despite having been first described nearly two centuries ago. To investigate these organs further, general trends in size of KO distribution and density were analyzed in hatchlings and juveniles of 17 octopod species from all oceans, representing holobenthic, holopelagic and meropelagic modes of life. The size of the KO is fairly constant across species, unrelated to mode of life or hatchling size. The density of KO is similar on ventral and dorsal body surfaces, but hatchlings of smaller size tend to have a higher density of KO on the aboral surface of the arms. Analysis of a series of post-hatching *Octopus vulgaris* shows KO size to be constant throughout ontogeny; it is therefore a consistent structure during the octopus early life from planktonic hatchling to benthic juvenile. New KO are generated on the skin of the arm tips during the planktonic period and initial benthic lives of juveniles. Their density, on both the mantle and arms, gradually decreases as the octopus grows. In older benthic juveniles, the KO degrades, losing its setae and the base of its follicle becomes exposed as a nearly circular stump of muscle. It is estimated that fully everted KO increase the body surface area by around two-thirds compared to when the KO are retracted. This modular mechanism of body surface extension and roughness probably influences flow-related forces such as drag and propulsion of the moving surface of the young octopus while it is of small size with a relatively large surface area. In addition, the distribution of these organs on the aboral surface of the arms of the octopus and their birefringent properties suggest a role in camouflage. Further research is needed to test these hypotheses of KO function in live animals.

**Keywords:** molluscs, cephalopod, larvae, juvenile, epidermis, buoyancy

## INTRODUCTION

Cephalopods have a uniform mode of early development: they all hatch with a complete set of internal organs and systems as in adults, including the gonads, that will develop when sexual maturation begins (Budelmann et al., 1997). However, the external morphology of some species changes notably during development: octopod embryos, hatchlings and juveniles have clumps of chitinous, bristle-like transitory structures, called Kölliker's organs (KO), present on the surface of the skin, which consequently has a punctate appearance (Figures 1, 2). These organs are present in species belonging to all three basic modes of octopod life, that is holobenthic, holopelagic and meropelagic (Lincoln et al., 1998). Why KO are absent from the other major cephalopod groups (cuttlefishes, squids, and nautilus) is unknown. These organs were originally described by Kölliker (1844) in embryos of *Argonauta argo* and subsequently their presence has been reported, illustrated or studied in 14 from the total of 55 octopod genera currently accepted (Table 1, Jereb et al., 2013). Through the development of transmission electronic microscopy, two major studies describing the general morphology of these intriguing organs were carried out by Boletzky (1973) and Brocco et al. (1974) who pointed out the similarities of KO setae with those of other invertebrate animals. The bristle-like setae or chaetae, are composed of longitudinally oriented filaments present in groups of lophotrochozoans such as annelids (Gustus and Cloney, 1973; Merz and Woodin, 2006); the mantle of brachiopods (Gustus and Cloney, 1972; Lüter, 2000); sensory organs of polyplacophoran molluscs (Leise and Cloney, 1982), and the gizzard teeth of bryozoans (Gordon, 1975). The chaetae or setae described for all these groups, including the KO of octopods, are similar but most probably not homologous structures (Hausen, 2005), with a huge range in the form, size and degree of arrangements. Here, we follow earlier studies on octopod KO (Boletzky, 1973; Brocco et al., 1974) by using the term *setae* to describe the simple, chitinous unit rodlets which make up the characteristic KO tuft.

Many hypotheses have been proposed to explain the possible function(s) of the KO, such as aids to buoyancy, support during hatching, defence or camouflage (Naef, 1923; Packard, 1988; Boletzky, 1978-1979; Villanueva and Norman, 2008) but none has been tested. Their function is obviously related to early octopus life, since they change form and disappear as the young octopus grows and are completely absent in subadult and adult octopod life stages. The development of these organs through the early octopus ontogeny is relatively well known since the embryonic development of KO was studied by Fioroni (1962). During embryo stage 24 (from a total of 30 embryonic stages) in *Octopus vulgaris*, several cells in the dermis differentiate into basal cells that will become the KO. Later, during stage 26, the basal cells of KO increase in number and form cup-shaped invaginations that secrete the setae of the KO (Nödl et al., 2015). KO are not merely residual structures from embryonic life that remain in the epidermis a few days after hatching, as does the hatching gland of cephalopods (Cyran et al., 2013). New KO continue to emerge from the skin after hatching until the developing octopus reaches the juvenile stage when it settles to the sea bottom.

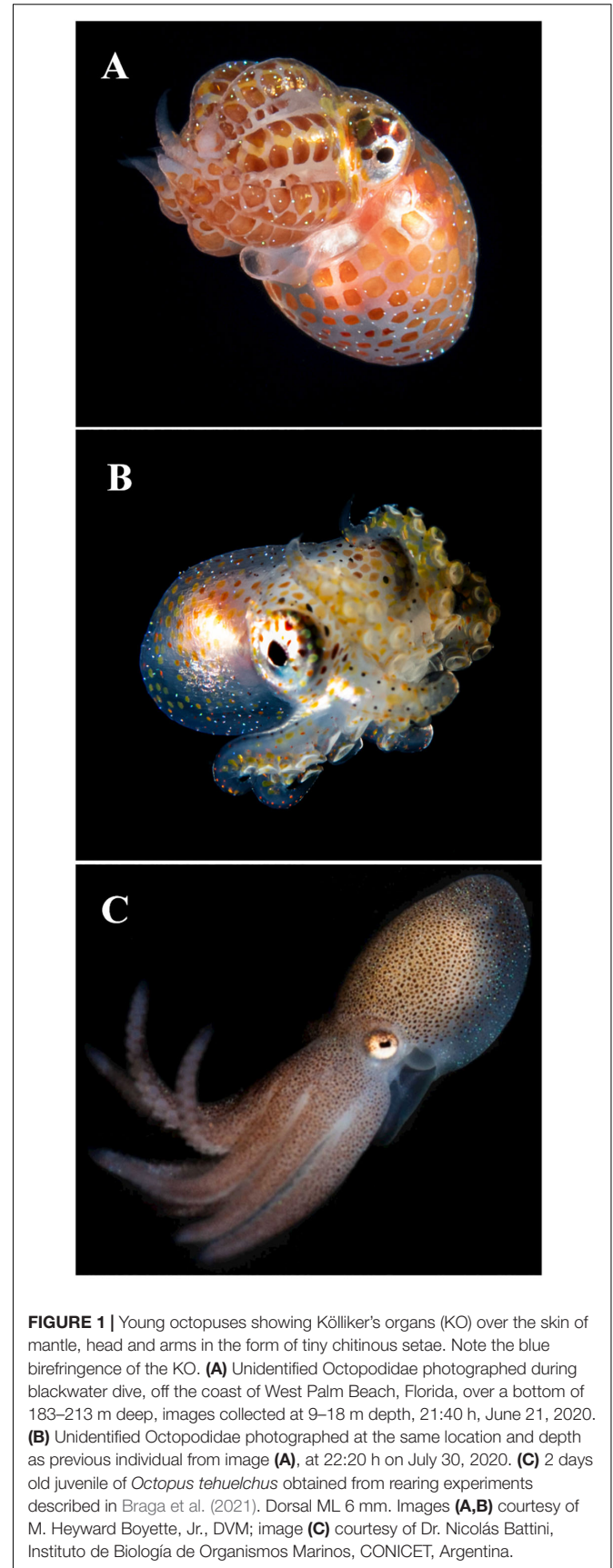
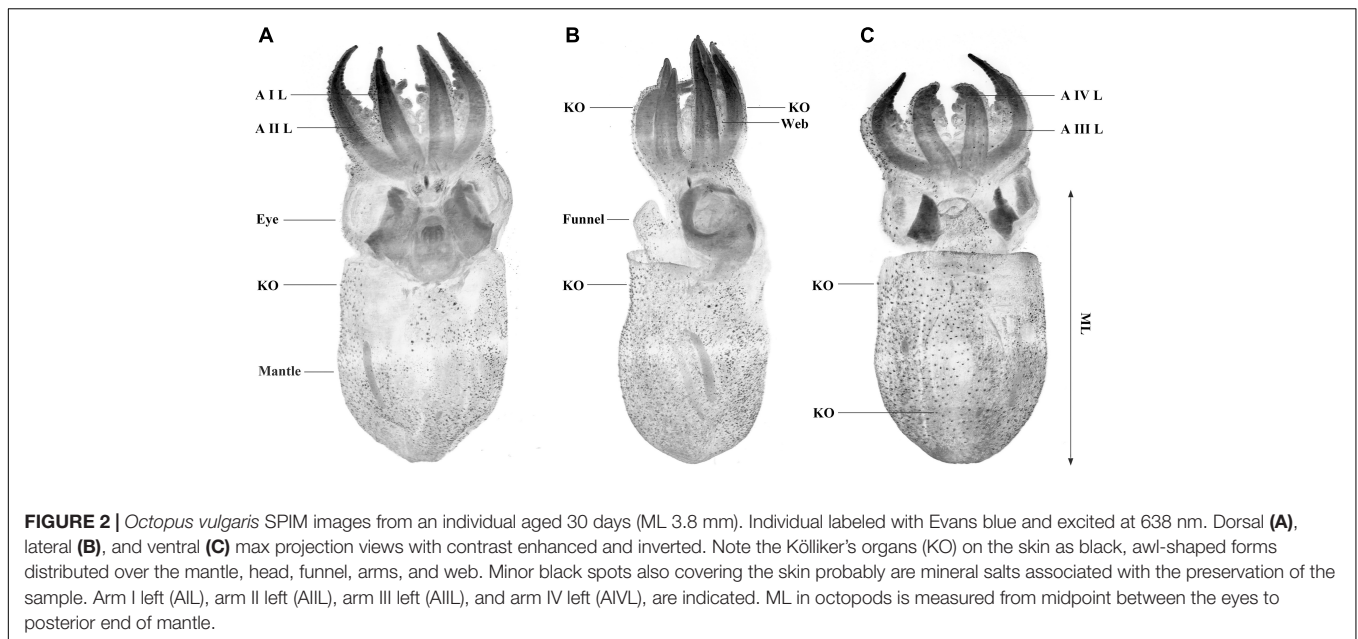


**FIGURE 1 |** Young octopuses showing Kölliker's organs (KO) over the skin of mantle, head and arms in the form of tiny chitinous setae. Note the blue birefringence of the KO. **(A)** Unidentified Octopodidae photographed during blackwater dive, off the coast of West Palm Beach, Florida, over a bottom of 183–213 m deep, images collected at 9–18 m depth, 21:40 h, June 21, 2020. **(B)** Unidentified Octopodidae photographed at the same location and depth as previous individual from image **(A)**, at 22:20 h on July 30, 2020. **(C)** 2 days old juvenile of *Octopus tehuilchus* obtained from rearing experiments described in Braga et al. (2021). Dorsal ML 6 mm. Images **(A,B)** courtesy of M. Heyward Boyette, Jr., DVM; image **(C)** courtesy of Dr. Nicolás Battini, Instituto de Biología de Organismos Marinos, CONICET, Argentina.



From rearing experiments with *O. vulgaris*, newly added KO have been observed in all stages, from hatchling to recently settled individuals, particularly over the new tissue formed at the tip of the rapidly growing arms (Villanueva and Norman, 2008). Despite detailed studies of KO ultrastructure and development, there is no information about the distribution and densities of KO over the octopus skin, nor studies evaluating interspecific variation, degradation or transformation processes associated with these organs toward the end of the octopod juvenile life. This study therefore addresses these deficiencies and for the first time a pattern is established, both for the KO size and spatial distribution by analysing the skin of hatchlings of 17 octopod species and investigating KO characteristics in *O. vulgaris* from hatchling to settled juveniles, when these structures disappear.

## MATERIALS AND METHODS

### Collection of Material

The material examined from 17 octopod species is listed in **Table 2**. Most hatchling individuals analyzed in the present study were collected from egg masses laid under laboratory conditions or in the field along with the brooding female, thus assuring the correct species identification of the hatchlings. The wild hatchlings of *Graneledone pacifica* are from Voight and Drazen (2004). The wild benthic juveniles of *Eledone cirrhosa* and *O. vulgaris* were collected in the NW Mediterranean from the commercial fishery during April and May 2018. To determine how the KO density pattern changes with animal age and growth, particular emphasis was given to the study of KO in *O. vulgaris*, using reared and wild specimens across a size range of 1.1 to 8.3 mm mantle length (ML) (**Table 2**). Individuals of *O. vulgaris* aged from 5 to 60 days are from rearing experiments described in Villanueva (1995); these

individuals were anesthetized in 2% ethanol as the temperature was lowered to approximately 3–4°C, fixed in buffered 2.5% formaldehyde and placed in long-term storage in 70% ethanol. Hatchlings of *O. vulgaris* and *O. maya* were fixed differently (see details in the following section on scanning electron microscope observations). Other individuals examined in the present study were anesthetized in 1.5–2% ethanol or by lowering the temperature to 3°C followed by formaldehyde fixation and storage in 70% ethanol. Currently accepted ethical procedures and recommendations for handling cephalopods in laboratory were followed (Fiorito et al., 2015).

### Observations With Scanning Electron Microscopy

For observations with Scanning Electron Microscopy (SEM), most samples were dehydrated through a series of ethanol solutions (80, 90, and 96%, absolute ethanol), each ethanol bath lasting 20 min. Samples were then critical-point dried using CO<sub>2</sub> as the transition liquid. Dehydration of some samples (*Amphioctopus aegina*, *Enteroctopus megalocyathus*, *Octopus tehuelchus*, and *Robsonella fontaniana*) was achieved by freeze-drying. Dried specimens were mounted on SEM stubs with double-sided adhesive conductive tape, with either the dorsal or ventral surface uppermost to expose the maximum body surface for observation; rarely, they were mounted to view the lateral surface or vertically to view the posterior mantle. Most mounted specimens were sputter-coated with gold–palladium or platinum for observation with a Hitachi S3500N, Hitachi SU3500 or JEOL JSM-T20 microscope. To obtain X-ray microanalysis of the KO, some dehydrated specimens were not sputter-coated, to avoid metal contamination. X-ray microanalysis of the KO was obtained by using an energy dispersive spectrometer (Thermo scientific UltraDry) coupled to a Hitachi SU3500 scanning electron microscope. This analysis was performed

**TABLE 1** | List of octopod species in which the presence or absence of Kölliker's organs (KO) have been reported.

Species	Mode of life	Presence/ Absence of KO	Life stage	Source
<i>Amphioctopus aegina</i>	MP	+	Hatchlings	Present study
<i>Amphioctopus burryi</i>	MP	+	Hatchlings	Packard, 1988
<i>Amphioctopus fangsiao</i>	HB	+	Hatchlings	Present study
<i>Argonauta argo</i>	HP	+	Embryos, hatchlings	Kölliker, 1844; Naef, 1923; Querner, 1927; Boletzky, 1973
<i>Argonauta hians</i>	HP	+	Hatchlings	Cyran et al., 2013; present study
<i>Bolitaena pygmaea</i>	HP	+	Not provided	Chun, 1915
<i>Callistoctopus macropus</i>	MP	+	Hatchlings	Naef, 1923; Boletzky et al., 2001, 2002
<i>Eledone cirrhosa</i>	MP	+	Hatchlings, juveniles	Mangold et al., 1971; Boletzky, 1973; present study
<i>Eledone moschata</i>	HB	+	Embryos, hatchlings	Boletzky, 1973
<i>Enteroctopus megalocyathus</i>	MP	+	Hatchlings	Ortiz et al., 2006; Villanueva and Norman, 2008; present study
<i>Graneledone pacifica</i>	HB	–	Hatchlings	Present study
<i>Hapalochlaena lunulata</i>	MP	+	Embryos	Overath and Boletzky, 1974
<i>Octopus briareus</i>	HB	–	Embryos, hatchlings	Boletzky, 1969, 1973, 1977
<i>Octopus hubbsorum</i>	MP	+	Hatchlings	Alejo-Plata and Herrera-Alejo, 2014
<i>Octopus incella</i>	MP	+	Hatchlings	Present study
<i>Octopus insularis</i>	MP	+	Embryos	Maldonado et al., 2019
<i>Octopus cf. joubini</i>	HB	+	Embryos, hatchlings	Boletzky, 1969
<i>Octopus maorum</i>	MP	+	Hatchlings	Batham, 1957
<i>Octopus maya</i>	HB	–	Hatchlings	Boletzky, 1973, 1977; present study
' <i>Octopus</i> ' <i>parvus</i>	MP	+	Hatchlings	Present study
<i>Octopus rubescens</i>	MP	+	Hatchlings	Brocco et al., 1974
<i>Octopus salutii</i>	MP	+	Hatchlings	Boletzky, 1973; Mangold-Wirz et al., 1976
<i>Octopus sinensis</i>	MP	+	Hatchlings	Present study
<i>Octopus tehuelchus</i>	HB	+	Hatchlings	Braga et al., 2021; present study
<i>Octopus cf. tetricus</i>	MP	+	Hatchlings	Joll, 1978
<i>Octopus vulgaris sensu stricto</i>	MP	+	Embryos, hatchlings, juveniles	Querner, 1927; Naef, 1928; Fioroni, 1962; Boletzky, 1973; Villanueva and Norman, 2008; Nödl et al., 2015; present study
<i>Pinnoctopus cordiformis</i>	MP	+	Hatchlings	present study
<i>Scaergus patagius</i>	MP	+	Hatchlings?	Young et al., 1989 as type F, then as <i>S. patagius</i> in Hochberg et al., 1992
<i>Scaergus unicolor</i>	MP	+	Embryos, hatchlings	Boletzky, 1984
<i>Robsonella fontaniana</i>	MP	+	Hatchlings	Ortiz and Ré, 2011; present study
<i>Robsonella huttoni</i>	MP	+	Hatchlings	Carrasco, 2014; present study
<i>Tremoctopus gelatus</i>	HP	+	Hatchlings	Nesis, 1979
<i>Tremoctopus gracilis</i>	HP	+	Hatchlings	Cyran et al., 2013; Mangold et al., 2018
<i>Tremoctopus violaceus</i>	HP	+	Hatchlings	Boletzky, 1973; Naef, 1923
<i>Tritaxeopus abaculus</i>	MP	+	Hatchlings	Present study
<i>Tritaxeopus aculeatus</i>	MP	+	Hatchlings	Present study
<i>Wunderpus photogenicus</i>	MP	+	Hatchlings	Huffard et al., 2009

Octopod mode of life: holobenthic (HB), holopelagic (HP), and meropelagic (MP), as well as life stage where KO were recorded, are indicated.

on KO *in situ* from specimens of *O. sinensis*, *O. tehuelchus*, *O. vulgaris*, *Pinnoctopus cordiformis*, *Robsonella huttoni*, and *Tritaxeopus aculeatus* (Supplementary Table 1). The specimens were not washed with distilled water before being fixed (except *O. vulgaris*, see below), therefore there may be an unquantified contribution of elements from seawater in the results. The mucus layer covering the skin surface in cephalopods is also observed in octopus hatchlings (Accogli et al., 2017). It apparently covers KO and prevents or hinders their detailed observation with SEM (see Results). Aiming to remove this mucus layer, glycerol was

used in preserved specimens before the ethanol dehydration step, as described for crustaceans (Felgenhauer, 1987), but there was no apparent improvement. Instead, a simple method to remove the mucus layer was used here with good results using fresh newly hatched individuals of *O. vulgaris* and *O. maya* reared in the laboratory during 2019 and 2020, respectively. Individuals of those two species were anesthetized in 2% ethanol, placed in a 500  $\mu\text{m}$  nylon net, then strongly flushed with distilled water for approximately 1 min to remove as much of the mucus layer as possible. They were then fixed in 96% ethanol.

**TABLE 2** | Material examined during the present study under SEM.

Species	n	Age (d)	ML (mm)	Oceanic distribution	Source
<i>Amphioctopus aegina</i>	7	0–7	1.5 ± 0.1	West Pacific	Promboon et al., 2011
<i>Amphioctopus fangsiao</i>	6	5–7	3.1 ± 0.3	NW Pacific	Hatched in laboratory; I. G. Gleadall
<i>Argonauta hians</i>	3	0	0.5 ± 0.0	Eastern Indian	Sukhsangchan and Nabhitabhata, 2007
<i>Eledone cirrhosa</i>	1	Unknown	16.8	NE Atlantic	Wild specimen, NW Mediterranean; R. Villanueva
<i>Enteroctopus megalocyathus</i>	3	0	4.3 ± 0.8	SW Atlantic	Ortiz et al., 2006
<i>Graneledone pacifica</i>	2	0	16, 17	NE Pacific	Voight and Drazen, 2004
<i>Octopus incella</i>	9	0	1.8 ± 0.1	NW Pacific	Hatched in laboratory; I. G. Gleadall
<i>Octopus maya</i>	6	0	5.2 ± 0.4	NW Atlantic	Hatched in laboratory; C. Rosas
' <i>Octopus</i> ' <i>parvus</i>	11	0–3	2.1 ± 0.2	NW Pacific	Hatched in laboratory; I. G. Gleadall
<i>Octopus sinensis</i>	6	12	1.0 ± 0.1	NW Pacific	Hatched in laboratory; I. G. Gleadall
<i>O. sinensis</i>	5	18	1.7 ± 0.1	NW Pacific	Hatched in laboratory; I. G. Gleadall
<i>Octopus tehuelchus</i>	3	0	4.5 ± 1.3	SW Atlantic	Hatched in laboratory; N. Ortiz
<i>Octopus vulgaris</i>	13	0	1.1 ± 0.1	NE Atlantic	Hatched in laboratory; R. Villanueva
<i>O. vulgaris</i>	1	5	1.2	NE Atlantic	Villanueva, 1995
<i>O. vulgaris</i>	1	10	1.4	NE Atlantic	Villanueva, 1995
<i>O. vulgaris</i>	3	19	2.7 ± 0.6	NE Atlantic	Villanueva, 1995
<i>O. vulgaris</i>	2	30	3.2, 3.6	NE Atlantic	Villanueva, 1995
<i>O. vulgaris</i>	1	42	4.1	NE Atlantic	Villanueva, 1995
<i>O. vulgaris</i>	1	46	3.9	NE Atlantic	Villanueva, 1995
<i>O. vulgaris</i>	3	50	5.3 ± 0.4	NE Atlantic	Villanueva, 1995
<i>O. vulgaris</i>	2	60	6.4, 7.0	NE Atlantic	Villanueva, 1995
<i>O. vulgaris</i>	4	Unknown	7.8 ± 0.4	NE Atlantic	Wild specimens, NW Mediterranean, O. Escolar
<i>Pinnoctopus cordiformis</i>	6	0	2.8 ± 0.2	SW Pacific	Carrasco, 2014
<i>Robsonella fontaniana</i>	3	0	1.9 ± 0.0	SW Atlantic	Ortiz and Ré, 2011
<i>Robsonella huttoni</i>	6	0	1.3 ± 0.2	SW Pacific	Carrasco, 2014
<i>Tritaxoopus abaculus</i>	6	0	1.0 ± 0.1	NW Pacific	Hatched in laboratory; I. G. Gleadall
<i>Tritaxoopus aculeatus</i>	6	0	1.5 ± 0.1	NW Pacific	Hatched in laboratory; I. G. Gleadall

The number of individuals (n), their age in days (d), and their mantle length (ML) after fixation are indicated as mean ± SD or the absolute value. The main oceanic distribution for each species and the source of material are also indicated.

## Observations With Selective Plane Illumination Microscopy

Newly hatched specimens of *O. vulgaris* were fixed in buffered 2.5% formaldehyde, stored in 70% ethanol and rehydrated to phosphate-buffered saline (PBS) progressively with a decreasing ethanol series (60, 40 and 20%) in PBS. After two washes in PBS, samples were incubated for 1 h at room temperature with 1% solution of 0.05% w/v Evans blue in PBS containing 0.01% Tween 20. After three washes with PBS, specimens were embedded in 1% low melting-point agarose and dehydrated in methanol following the procedure of Quintana and Sharpe (2011), then chemically cleared with BABB (benzyl alcohol and benzyl benzoate, mixed in the ratio 1:2). Each embedded octopus was immersed in a BABB-filled chamber for Selective Plane Illumination Microscopy (SPIM) imaging, which was performed using a 5×/0.12 NA air objective lens (Leica N PLAN EPI) for detection and a 2.5×/0.07 NA air objective lens (Leica N PLAN) for illumination. A Hamamatsu Orca-ER camera was used to record images. In the custom-built SPIM system used here (Swoger et al., 2011), the microscope components are controlled with Labview (National Instruments). Autofluorescence was excited with a 488 nm diode laser and detected using a 525/50 bandpass filter. For the Evans blue channel, excitation was with

a 638 nm diode laser and detection was with a 700/75 bandpass filter. The 0 day *O. vulgaris* was not labeled with Evans blue and its autofluorescence was excited at 638 nm. Each tile represents a field of view of 1321 μm × 1734 μm. For the newly hatched octopus two tiles were required, with a z-stack of 237 planes; 30-day old octopus, 15 tiles and a z-stack of 561 planes; and for the 50-day old octopus, 32 tiles and a z-stack of 881 planes. The spacing of slices in the z-stacks was 5 μm. All data processing, from stitching the tiles to down-sampling was done with the open-source software Fiji (Schindelin et al., 2012).

## Estimation of Size, Distribution and Density of KO

Terminology applied to the different KO elements and general appearance follow Brocco et al. (1974). The three principal parts of the KO are: a follicle of specialized epidermal cells; an extracellular fascicle of setae (cannular rodlets forming the KO tuft); and a group of obliquely striated dermal muscle fibers (see Figure 12 in Brocco et al., 1974). The KO was considered *erupted* when the setae are compacted together, distally tapered and protruding from the skin surface (Figures 3A,B,E); and *everted* when the base of the follicle has been raised, causing the setae separate and splay into a patulous array over the

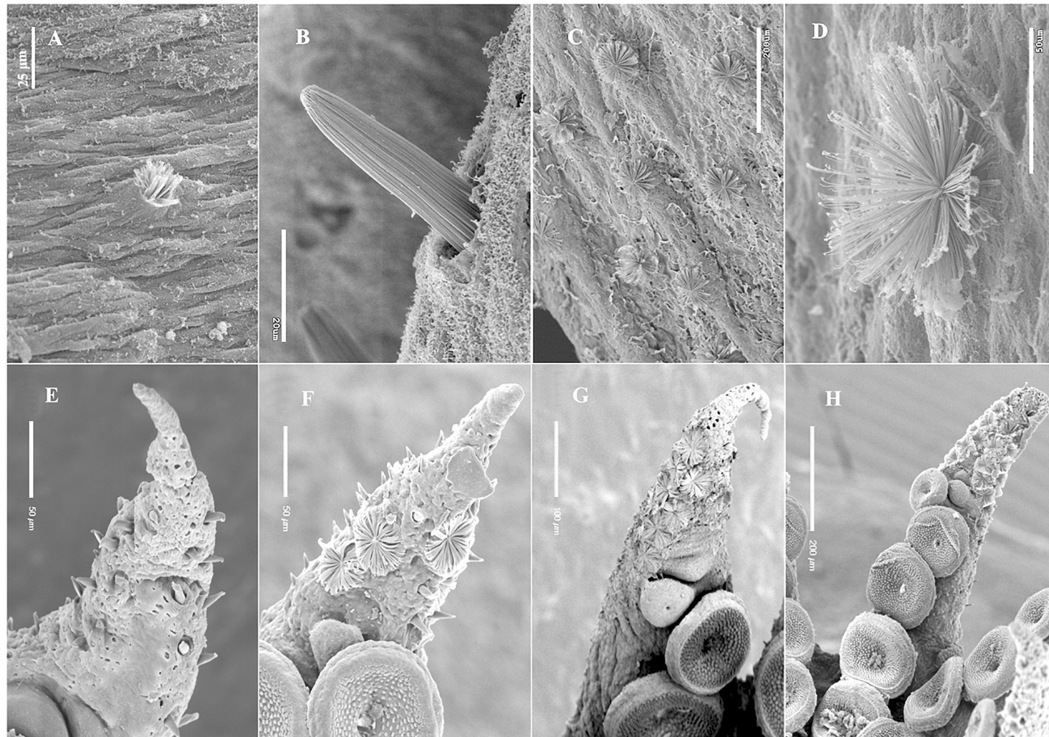


**FIGURE 3** | Kölliker's organs (KO) eruption and eversion sequence, SEM images. **(A)** Initially erupted KO on the dorsal mantle, *Amphiocotopus fangsiao*, aged 5 days, (ML 3.2 mm); **(B)**, erupted KO on the dorsal surface of right arm II, *Enterocotopus megalocyathus*, 5.3 mm ML, aged 0 day; **(C)**, several fully everted KO, ventral mantle, *Octopus vulgaris*, wild benthic individual 7.8 mm ML; **(D)**, detail of fully everted KO on dorsal mantle of the same individual as in **(C)**. **(E–H)** *Amphiocotopus aegina*, arm tips with KO on the arm oral side. Note that setae from contiguous KO can be in contact when fully everted. **(E)** KO erupted (none everted) on right arm IV from an individual aged 0 day; **(F)**, KO erupted and everted on right, arm II, from an individual aged 7 days; **(G)**, most KO everted on right arm II of an individual aged 2 days; **(H)**, most KO everted on right arm I of an individual aged 3 days.

epidermis (**Figures 3C,D,E,G**). KO size was defined by the seta length (SL), measured from all everted KO observed, using the image processing program ImageJ. To estimate changes in surface area when a KO is fully everted, in comparison with its completely retracted state under the skin, the external surface and volume of a fully everted KO were estimated, assuming the formation of a hemisphere of radius SL (**Figures 3D,E,G,H, 4C,D,F,H, 5D, 6G,H**). Accordingly, to estimate the everted Kölliker's organ volume (EKOV) and the everted Kölliker's organ surface (EKOS), the following formulae were used:

$$\text{EKOV} = 2/3\pi\text{SL}^3$$

$$\text{EKOS} = 2\pi\text{SL}^2$$

The surface area of a hemisphere is twice the area of its two-dimensional cross-sectional area ( $\pi\text{SL}^2$ ), so the surface area described by the tips of the splayed setae of a fully everted KO doubles the surface area of the skin over which it is splayed. For each species, the maximum surface-area increase due to full KO eversion was calculated for a unit skin area ( $1\text{ mm}^2$ ), as a percent increase compared to when KO are fully retracted within their follicle (i.e., invaginated). This maximum increased surface area was calculated using the SL of the species and its KO density

obtained for this unit area (see below). KO distribution on the skin of the octopus was assessed for the aboral surface of the arms versus the mantle, head and funnel, each assessed for their dorsal and ventral component surfaces. For the arms, “dorsal” refers to the dorsal and dorsolateral arm pairs (arm pairs I and II), and “ventral” refers to the ventrolateral and ventral arm pairs (arm pairs III and IV). To estimate the density of KO per  $\text{mm}^2$  from the SEM images, only well-defined skin areas with clearly identified KO erupted and/or everted, were selected as Counting Areas (CA). As indicated above, the octopus skin was sometimes covered with a mucus layer over extensive regions, preventing KO observation. All the KO observed inside a square of known surface area were counted, using the software ImageJ. Each examined square surface was adjusted to the magnification of the image and an attempt was made to count all possible areas where KO were observed, avoiding overlapping areas. CA selected to obtain KO density included those of different degrees of setae extension. The total surface of the CA used to count KO ranged from  $10.000$  to  $900.000\text{ mm}^2$  (mean =  $48.971\text{ mm}^2$ ; SD =  $62.533$ ). The individuals, KO densities and number of CA used are indicated in **Supplementary Table 2**. In addition to the 17 species analyzed here, published information on KO size and/or density in three other species was included. For *Octopus rubescens*, the SL provided by Brocco et al. (1974) was

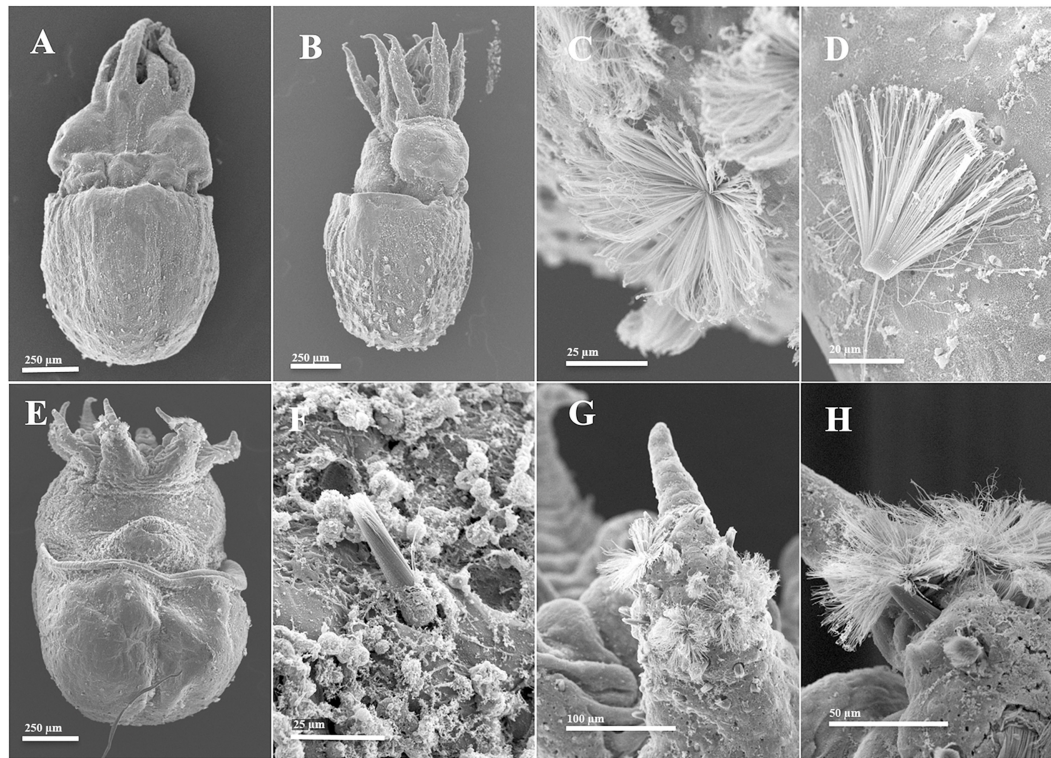


**FIGURE 4 |** *Tritaxoepus abaculus* hatchlings (**A–D**) and *Octopus sinensis*, age 12 days (**E–H**) SEM images. (**A**) dorsal view (ML 1.1 mm). Note erupted Kölliker's organs (KO) on the mantle with their axis oriented obliquely with reference to the surface of the skin and directed anteriorly. Note also conspicuous dorsal line on each side close to midline, from head along arm I; (**B**) left lateral view (1.0 mm ML). Note everted KO on mantle surface and erupted KO over the arms; (**C**) detail of everted KO over the ventral mantle (same individual as **B**); (**D**) tuft of ejected setae lying on ventral surface of head (ML 1.0 mm) possibly a handling artifact. (**E**) Ventral view (ML 0.9 mm) showing erupted KO on mantle, funnel, head and arms, and everted KO on ventral arms; (**F**) erupted KO on dorsal surface of head (ML 1.1 mm); (**G,H**), detail of erupted and everted KO on tip of right (**G**) and left (**H**) ventral arms from the individual of image (**E**).

used and its KO density on the mantle was estimated from their **Figure 2** (note that the species was originally identified to genus only, as *Octopus* sp., but was subsequently identified as *O. rubescens* by Hochberg et al., 1992). The SL and KO density of *E. moschata* were estimated from Boletzky (1973; Figure 1); and SL for *Octopus* cf. *tetricus* from Joll (1978; Figure 6). The ML of the *E. cirrhosa* preserved hatchling reported by Mangold et al. (1971) was estimated to be 3.3 mm from their fresh ML of 4.5 mm, applying 25.8% mean shrinkage reported for hatchlings from five cephalopod species (Villanueva et al., 2016).

## Data Treatment

Inter- and intraspecific values of KO size, distribution and density were compared using simple and paired Student's *t*-test and correlation test. Differences were considered significant when  $p < 0.05$ . Data were assessed using the JMP statistical package.

## RESULTS

### Form and Structure of KO

A total of 120 individuals belonging to 17 octopod species were examined successfully by SEM during the present study

(**Table 2**) and three individuals of *O. vulgaris* by SPIM. KO were present in all species except in the holobenthic species *G. pacifica* and *O. maya*. External morphology of the KO examined matched those described in previous studies (Boletzky, 1973; Brocco et al., 1974). In all species, most of the observed KO showed erupted tufts (**Figures 4E**, **Figures 5A–C,E–G**, **6A–D**) and only in a few KO from each species the cannular setae were fully everted and radiating onto the epidermis (**Table 3** and **Figures 4B,C,H**, **5D,H**, **6G,H**). Erupted KO tufts are tapered (with awl-shaped tips), with their axes oriented obliquely with reference to the skin surface and directed anteriorly (i.e., **Figures 4A**, **7**). It was possible to observe erupted and everted KO very close to each other. Moreover, when several KO are everted in close proximity, the distal ends of their setae can be in contact, making it possible for the extended setae to cover much of the skin surface (**Figures 3F,G,H**, **4C,G,H**). Investigation of the elemental composition of the KO shows that the major elements (excluding C, N, and O) are sulfur and phosphorous along with calcium and sodium (**Supplementary Table 1**).

### Distribution and Density of KO

In the species examined, the KO were distributed on the external epidermis of both the dorsal and ventral surfaces of the mantle,

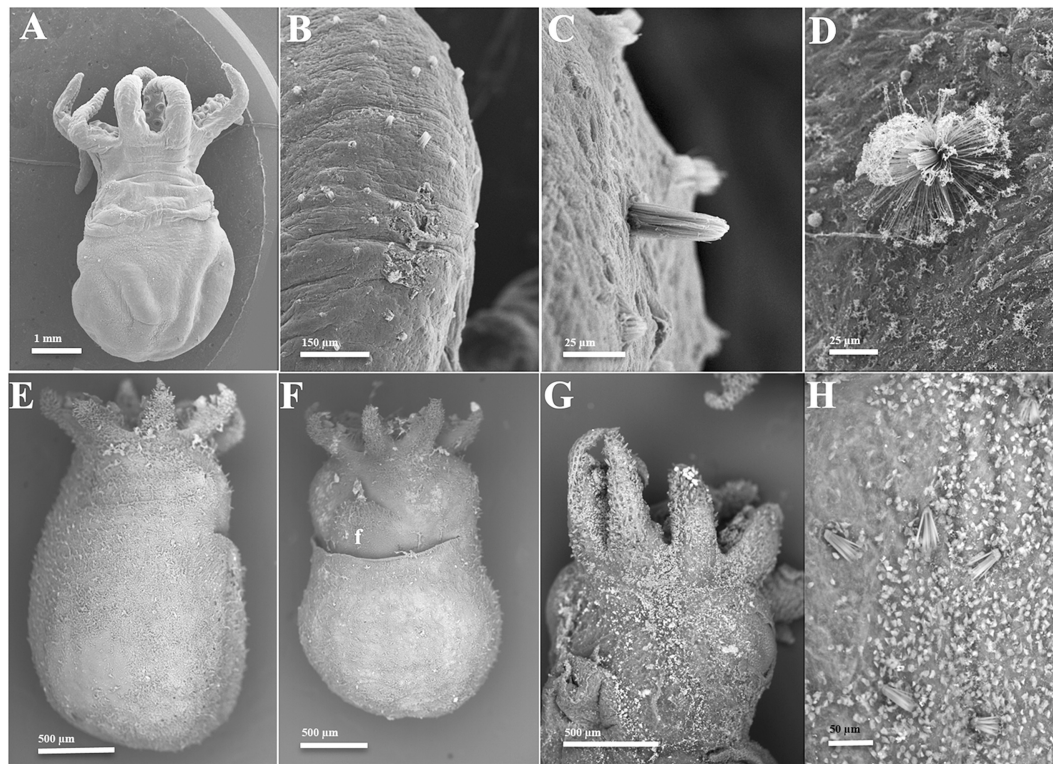


**FIGURE 5 |** Scanning Electron Microscopy images of **(A–D)** *Amphioctopus fangsiao* (5 days, ML 3.2 mm); **(E,F)** *Robsonella fontaniana* (two individuals, both 0 day, ML 1.9 mm) and **(G,H)** *Pinnoctopus cordiformis* (two individuals, both 0 day, 2.6 mm ML). **(A)** Dorsal view; **(B)** initially erupted and semi-erupted KO on right arm I; **(C)** KO erupted on left arm I; **(D)** everted KO on dorsal mantle; **(E)** dorsal view; **(F)** ventral view. Note density of erupted KO on distal funnel (f); **(G)**, ventral view; **(H)** everted KO on ventral mantle.

funnel, head, eyelid and aboral surface of all arms. KO were typically absent from the oral surface of the arms, web, and the suckers, including the sucker rim and infundibulum. The arm tips usually lacked KO in most species probably because of the active and fast growth of this tissue. The only exception was *A. aegina*, where KO were observed on both the oral and aboral arm tip (Figures 3E–H). When comparing KO densities on the arms versus the mantle + head, and ventral surface versus dorsal surface of the whole animal, in the hatchlings of seven species (*A. aegina*, *O. sinensis*, *O. vulgaris*, *P. cordiformis*, *R. fontaniana*, *R. huttoni*, and *T. abaculus*), KO density was higher in the arms than in mantle + head (paired *t*-test,  $p < 0.033$ ) but did not differ between ventral and dorsal whole animal surfaces (*t*-test,  $p > 0.1$ ). In the remaining three species (*A. fangsiao*, *E. megalocyathus*, and *O. tehuelchus*), no differences in density were found between the arms and mantle + head (paired *t*-test,  $p > 0.3$ ), with *E. megalocyathus* showing higher KO density ventrally (*t*-test,  $p = 0.03$ ) and *O. tehuelchus* dorsally (*t*-test,  $p < 0.01$ ; Table 3 and Figures 8C,D). No significant correlation was observed between hatchling ML and KO density on the mantle and head ( $n = 13$  species,  $r^2 = 0.04$ ,  $p > 0.9$ ); but these characters were negatively correlated on the arms ( $n = 11$  species,  $r^2 = 0.67$ ,  $p < 0.03$ ) (Figures 8A,B). In newly hatched *O. vulgaris* ( $n = 13$  individuals), when the whole (mantle, head and arms) dorsal and ventral KO densities were compared, no differences were observed (*t*-test,  $p > 0.6$ ). However, on the mantle alone, significantly higher

densities were found dorsally ( $566 \pm 101$  KO  $\text{mm}^{-2}$ ) than ventrally ( $474 \pm 96$  KO  $\text{mm}^{-2}$ ), (*t*-test,  $p = 0.0004$ ). In this species, as the animal grows, KO density both on the arms and mantle + head has decreased nearly 10-fold when the animals have reached around 4 mm ML (Table 3 and Figures 9A,B). Throughout the planktonic period and beginning of benthic life, KO densities on the arms continued to be higher than or equal to those of the rest of the body, although comparisons between ventral and dorsal varied (Table 3). Although apparently in small and undetermined numbers, new KO are generated from hatching to settlement in *O. vulgaris*, at least on the aboral side of the arms during planktonic life (Figure 10). These KO can be recognized easily as post-hatching KO because *O. vulgaris* has short arms at hatching with only three suckers per arm and the arms then grow allometrically with the actively growing zone at the tip of the arms of specimens that have grown to the 30-sucker stage, and in benthic juveniles with 52 suckers, so these KO definitely were not present at hatching. In contrast, on the mantle, using SEM it was not possible to discern old versus new KO added after hatching because of the lack of any definitive growth points.

### Size and Surface of KO

The everted KO allowed the seta length (SL) in all species to be determined, except for *T. aculeatus* where only a few

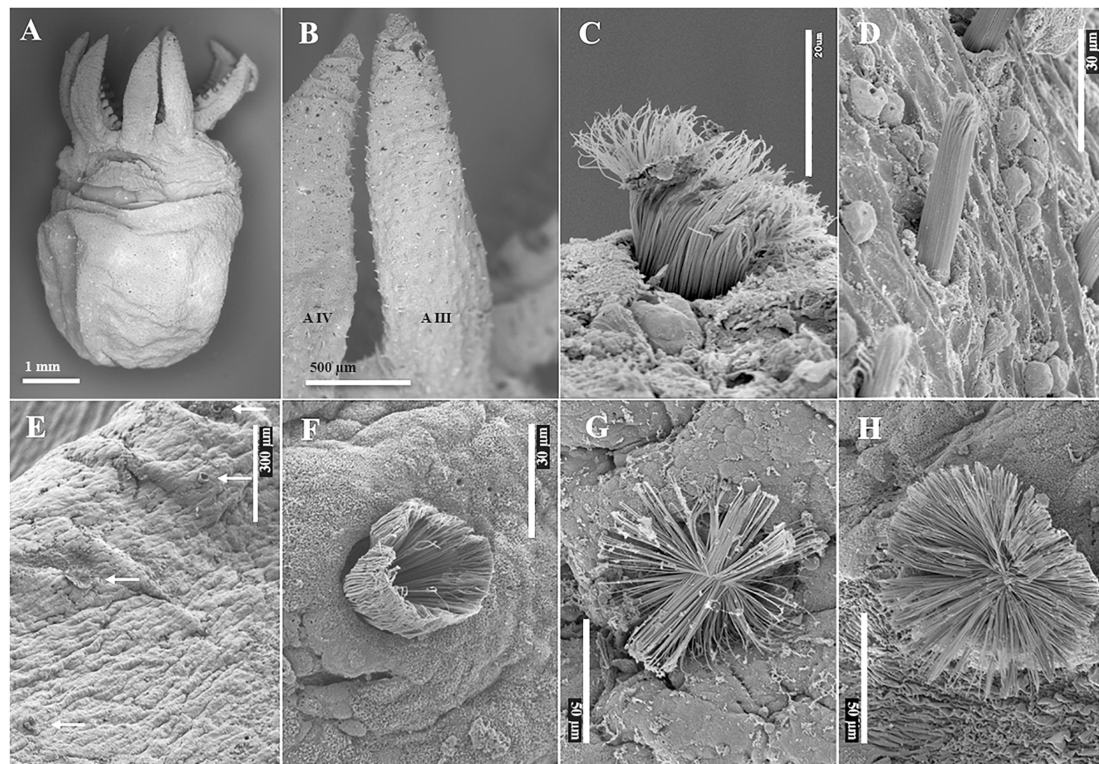


**FIGURE 6 |** Scanning Electron Microscopy images of hatching *Enteroctopus megalocyathus* (**A,B**, ML 3.8 mm; **C,D**, ML 5.3 mm) and wild benthic juvenile 16.8 mm ML *Eledone cirrhosa* (**E–H**). (**A**) ventral view; (**B**) detail of left arms III (AIII) and IV (AIV), showing erupted Kölliker's organs (KO); (**C**) semi-erupted KO on dorsum of head; (**D**) erupted KO on dorsal surface of right arm II. (**E**) Semi-erupted and everted KO (white arrows) on left arm III; (**F**) details of semi-erupted KO; (**G,H**) fully everted KO.

erupted KO tufts were observed. The number of everted KO from which it was possible to measure the representative SL for each species was always low, ranging from only two in *O. parvus* and *R. fontaniana* to 38 in *O. vulgaris* (Table 3). The mean SL ranged from  $27.5 \pm 2.1 \mu\text{m}$  in *A. aegina* to  $49.5 \pm 1.0 \mu\text{m}$  in *T. abaculus*. Accordingly, estimates of surface area and volume of a fully everted KO ranged from 4,741 to 15,395  $\mu\text{m}^2$  and from 43,408 to 254,018  $\mu\text{m}^3$  for *A. aegina* and *T. abaculus*, respectively (Tables 3, 4). The relationship between hatchling ML and SL for all the available species pooled ( $n = 17$ ) showed no correlation ( $r^2 = 0.26$ ,  $p > 0.3$ ; Figure 9C). In newly hatched *O. vulgaris*, no everted KO were found; the SL of individuals aged 5 days was of  $46.6 \pm 0.5 \mu\text{m}$ . A very uniformly sized SL through the early life of the animal (i.e., from planktonic hatching to benthic juvenile), ranging from  $46.6 \pm 0.5$  to  $47.6 \pm 2.6 \mu\text{m}$  was found in *O. vulgaris* (Table 3). The linear fit between ML and SL for the individuals of this species ( $n = 7$ ; 1.2 to 8.3 mm ML; Table 3) was uncorrelated ( $r^2 = 0.29$ ,  $p > 0.5$ ). In addition, SL in *O. vulgaris* showed no significant differences when comparing all SL from dorsal ( $46.7 \pm 2.1 \mu\text{m}$ ) versus all SL from ventral surfaces ( $47.2 \pm 0.9 \mu\text{m}$ ) ( $t$ -test,  $p > 0.4$ ). Similarly, no differences were recorded when comparing all SL from the arms ( $46.8 \pm 2.1 \mu\text{m}$ ) versus all SL from the mantle + head ( $46.9 \pm 1.6 \mu\text{m}$ ) ( $t$ -test,  $p > 0.8$ ), indicating that KO are relatively uniform in size on all surfaces. Fully everted KO increased the body surface of the

octopus. In hatchlings, the estimated increase ranged from 35% on the ventral surface of *O. tehuelchus* to 87% on the arms of *Tritaxoepus abaculus* (Table 4). When hatchlings of all species were pooled, the mean increase in body surface area when KO were fully everted represented  $67 \pm 14\%$  of the body surface area in comparison to when KO are retracted under the skin.

## Degradation and Loss of KO in Advanced Juveniles

In a wild benthic juvenile *E. cirrhosa*, some isolated and everted KO were observed on the head, funnel and arms (Figures 6E,F). This is the largest octopod with KO encountered during the present study (16.8 mm ML after dehydration for SEM; 23.2 mm fresh ML, 2.9 g fresh weight). Apparent degradation of KO was observed over the dorsal mantle skin of *O. vulgaris* in advanced benthic juveniles of 7.3, 7.6 and 7.8 mm ML. This degradation was characterized by the gradual loss of the cannular setae and the exposure of the basal KO follicle in the form of a near-circular muscle stump  $27.1 \pm 2.3 \mu\text{m}$  in maximum diameter (Figures 11E,F). Clusters of muscle stumps were found mixed with everted, apparently functional KO (Figure 11B). This phenomenon is probably not an artifact of fixation because muscle stumps were observed only in the larger specimens examined.

**TABLE 3** | Kölliker's organs (KO) density and seta length. Density (mean  $\pm$  SD no. of KO per mm<sup>2</sup>) on the mantle + head, arms and on the ventral and dorsal surface of the individuals are indicated.

Species	N	Age (d)	Mantle + head	CA (n)	Arms	CA (n)	Ventral surface	CA (n)	Dorsal surface	CA (n)	Seta length ( $\mu$ m)	EKO (n)	Ind. with EKO (n)	ML ind. with EKO (mm)
<i>Amphioctopus aegina</i>	7	0–7	659 $\pm$ 158 <sup>a</sup>	17	863 $\pm$ 295 <sup>b</sup>	11	754 $\pm$ 330 <sup>a</sup>	10	733 $\pm$ 199 <sup>a</sup>	18	27.5 $\pm$ 2.1	16	3	1.5 $\pm$ 0.1
<i>Amphioctopus fangsiao</i>	6	5–7	194 $\pm$ 185 <sup>a</sup>	28	142 $\pm$ 123 <sup>a</sup>	22	–	–	171 $\pm$ 161	50	48.1 $\pm$ 3.5	19	3	3.1 $\pm$ 0.2
<i>Argonauta hians</i>	3	0	283 $\pm$ 188	3	300	1	400 $\pm$ 141	2	175 $\pm$ 0	2	38.8 $\pm$ 1.3	3	2	0.5, 0.5
<i>Eledone cirrhosa</i>	1	?	–	–	–	–	–	–	–	–	48.0 $\pm$ 1.3	3	1	16.8
<i>Enteroctopus megalocyathus</i>	3	0	166 $\pm$ 89 <sup>a</sup>	75	173 $\pm$ 56 <sup>a</sup>	35	143 $\pm$ 48 <sup>a</sup>	32	179 $\pm$ 88 <sup>b</sup>	78	43.7 $\pm$ 3.6	4	2	3.8, 5.3
<i>Octopus incella</i>	9	0	–	–	–	–	–	–	–	–	38.5 $\pm$ 7.7	3	2	1.6, 1.8
<i>'Octopus' parvus</i>	11	0–3	–	–	–	–	–	–	–	–	44.6	2	2	2.0, 2.1
<i>Octopus sinensis</i>	6	12	706 $\pm$ 464 <sup>a</sup>	18	1037 $\pm$ 411 <sup>b</sup>	18	872 $\pm$ 474 <sup>a</sup>	29	871 $\pm$ 178 <sup>a</sup>	7	43.5 $\pm$ 3.7	5	2	0.9, 1.1
<i>O. sinensis</i>	5	18	174 $\pm$ 125 <sup>a</sup>	15	523 $\pm$ 189 <sup>b</sup>	14	419 $\pm$ 271 <sup>a</sup>	7	318 $\pm$ 225 <sup>a</sup>	22	–	–	–	–
<i>Octopus tehuelchus</i>	3	0	587 $\pm$ 403 <sup>a</sup>	15	522 $\pm$ 285 <sup>a</sup>	8	86 $\pm$ 65 <sup>a</sup>	4	665 $\pm$ 311 <sup>b</sup>	19	44.6 $\pm$ 4.1	4	2	3.6, 6.0
<i>Octopus vulgaris</i>	13	0	498 $\pm$ 136 <sup>a</sup>	95	823 $\pm$ 261 <sup>b</sup>	72	645 $\pm$ 238 <sup>a</sup>	83	631 $\pm$ 274 <sup>a</sup>	84	–	–	–	–
<i>O. vulgaris</i>	1	5	500 $\pm$ 67	12	500 $\pm$ 141	2	500 $\pm$ 74	14	–	–	46.6 $\pm$ 0.5	3	1	1.2
<i>O. vulgaris</i>	1	10	425 $\pm$ 50	4	400	1	–	–	420 $\pm$ 45	5	–	–	–	–
<i>O. vulgaris</i>	3	19	238 $\pm$ 123 <sup>a</sup>	30	613 $\pm$ 76 <sup>b</sup>	8	238 $\pm$ 54 <sup>a</sup>	12	353 $\pm$ 198 <sup>b</sup>	26	–	–	–	–
<i>O. vulgaris</i>	2	30	129 $\pm$ 34 <sup>a</sup>	26	269 $\pm$ 55 <sup>b</sup>	4	136 $\pm$ 35 <sup>a</sup>	19	168 $\pm$ 87 <sup>a</sup>	11	–	–	–	–
<i>O. vulgaris</i>	1	42	76 $\pm$ 27 <sup>a</sup>	15	74 $\pm$ 6 <sup>a</sup>	3	96 $\pm$ 6 <sup>a</sup>	5	68 $\pm$ 24 <sup>b</sup>	13	47.5 $\pm$ 0.9	7	1	4.1
<i>O. vulgaris</i>	1	46	41 $\pm$ 3 <sup>a</sup>	5	55 $\pm$ 6 <sup>b</sup>	4	–	–	47 $\pm$ 8	9	–	–	–	–
<i>O. vulgaris</i>	3	50	58 $\pm$ 24 <sup>a</sup>	34	47 $\pm$ 20 <sup>a</sup>	10	63 $\pm$ 29 <sup>a</sup>	21	49 $\pm$ 15 <sup>b</sup>	23	47.6 $\pm$ 2.6	8	1	5.2
<i>O. vulgaris</i>	2	60	33 $\pm$ 15 <sup>a</sup>	14	38 $\pm$ 14 <sup>a</sup>	6	37 $\pm$ 13 <sup>a</sup>	18	13 $\pm$ 9 <sup>b</sup>	2	–	–	–	–
<i>O. vulgaris</i>	4	?	12 $\pm$ 4 <sup>a</sup>	25	17 $\pm$ 6 <sup>b</sup>	10	13 $\pm$ 5 <sup>a</sup>	28	14 $\pm$ 5 <sup>a</sup>	7	46.7 $\pm$ 2.0	20	4	7.8 $\pm$ 0.4
<i>Pinnoctopus cordiformis</i>	6	0	130 $\pm$ 147 <sup>a</sup>	7	661 $\pm$ 453 <sup>b</sup>	23	606 $\pm$ 97 <sup>a</sup>	22	349 $\pm$ 321 <sup>a</sup>	8	43.0 $\pm$ 2.1	5	3	2.7 $\pm$ 0.2
<i>Robsonella fontaniana</i>	3	0	171 $\pm$ 39 <sup>a</sup>	20	916 $\pm$ 183 <sup>b</sup>	8	422 $\pm$ 411 <sup>a</sup>	15	341 $\pm$ 100 <sup>a</sup>	13	48.5	2	1	1.9
<i>Robsonella huttoni</i>	6	0	102 $\pm$ 36 <sup>a</sup>	7	785 $\pm$ 418 <sup>b</sup>	10	567 $\pm$ 279 <sup>a</sup>	6	470 $\pm$ 554 <sup>a</sup>	11	46.9 $\pm$ 1.4	4	2	1.5, 1.5
<i>Tritaxoopus abaculus</i>	6	0	245 $\pm$ 51 <sup>a</sup>	11	450 $\pm$ 187 <sup>b</sup>	6	333 $\pm$ 170 <sup>a</sup>	13	269 $\pm$ 38 <sup>a</sup>	4	49.5 $\pm$ 1.0	3	1	1.1

Density values with different superscript letters denote statistically significant differences between the pair (comparing mantle + head vs arms, and ventral vs dorsal surface) denote statistically significant differences between the pair (Student-t,  $p < 0.05$ ). The number of counting areas (CA) used to estimate KO densities for each skin zone is indicated (n). Values for species with three or less available CA were not compared. Mean  $\pm$  SD seta length (SL), everted Kölliker's organs (EKO) observed and number and size (mantle length, ML) of individuals with everted KO are indicated. N, total number of individuals examined; d, age in days. Individuals marked with unknown age (?) correspond to wild benthic specimens, including one *E. cirrhosa* (i.e., 16.8 mm mantle length, ML) and four *O. vulgaris* (7.3–8.3 mm ML).

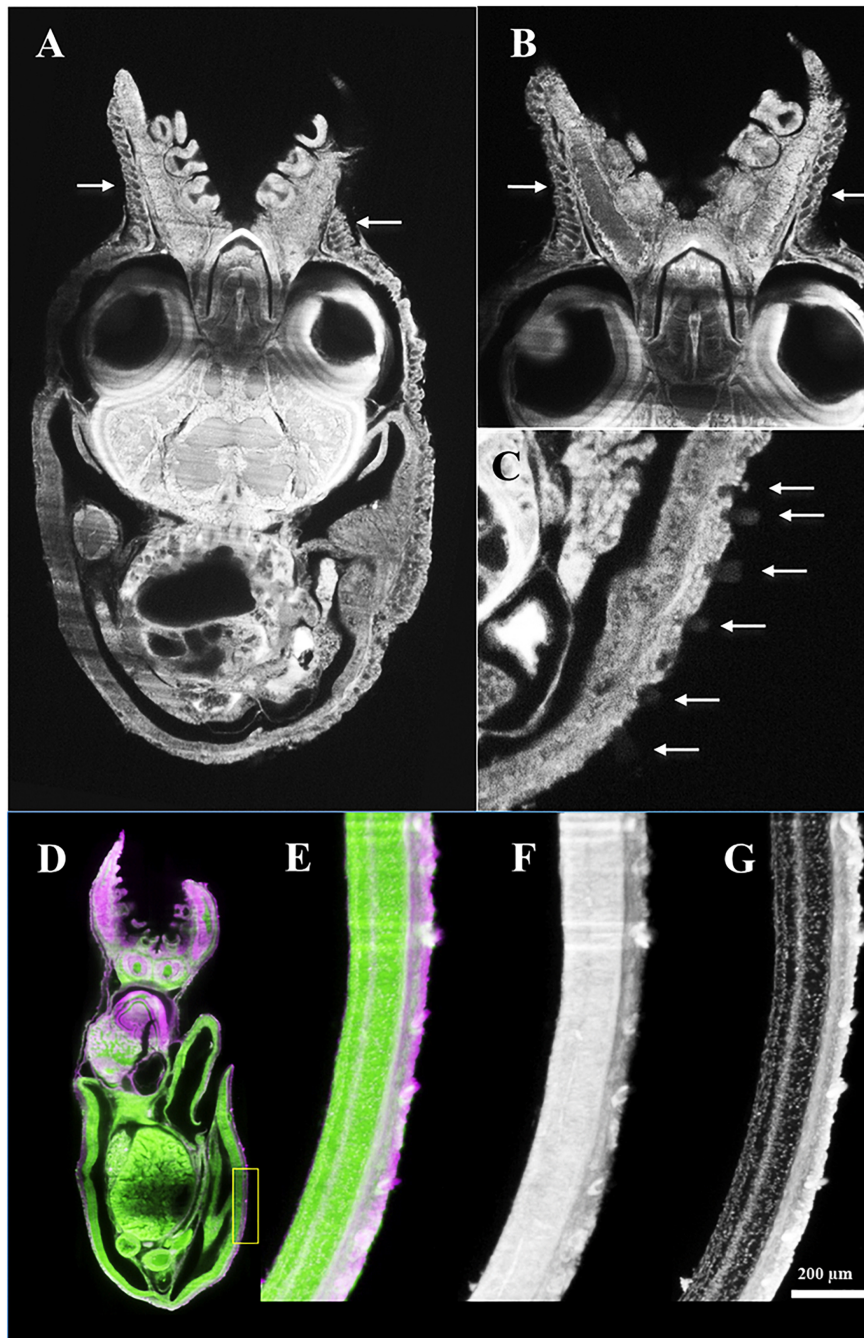
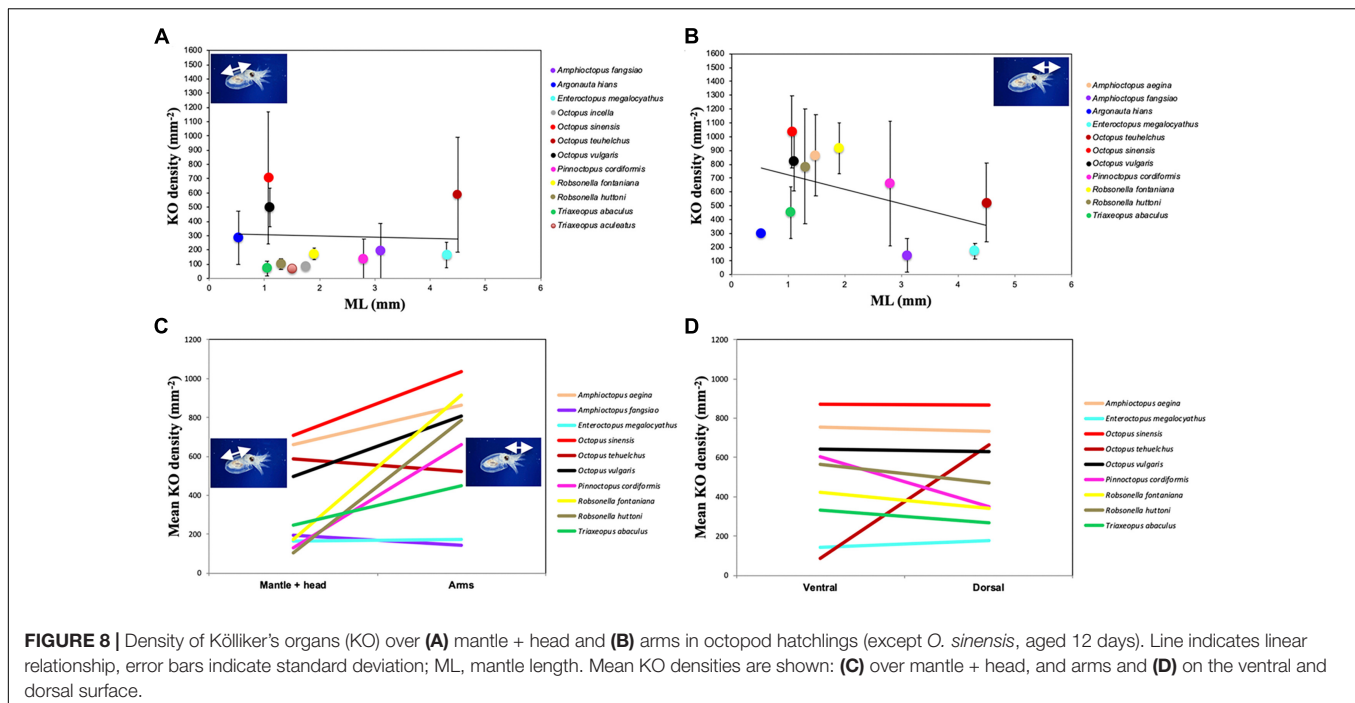


**FIGURE 7** | *Octopus vulgaris* SPIM images. **(A–C)** age 0 day, ML 1.6 mm, horizontal section, autofluorescence image excited at 638 nm; and **(D–G)** 30 days, ML 3.8 mm, sagittal section, labeled with Evans blue and excited at 638 nm (pink color) and autofluorescence excited at 488 nm (green color). Note high density of Kölliker's organs (KO) (white arrows) on skin of aboral arm **(A,B)** in comparison with mantle surface **(C)**. **(D)** Whole animal and detail of the ventral mantle (inside yellow rectangle) showing KO under different excitation conditions: **(E)** autofluorescence + Evans blue, **(F)** autofluorescence, and **(G)** Evans blue.

## DISCUSSION

The external morphology of the KO examined matched that described in previous studies, following the erupted-everted sequence exposing the KO tuft and setae to the external environment. Everted KO were generally present in very low

numbers, close to erupted ones, suggesting that control of eruption/eversion is independent for each KO. Boletzky (1973) noted that in fresh tissue of *Eledone moschata* hatchlings, the cycle of eruption, eversion and retraction of KO took a duration of 1 s and the appearance of this process was spaced at irregular intervals. The physical or chemical stimulus and/or associated



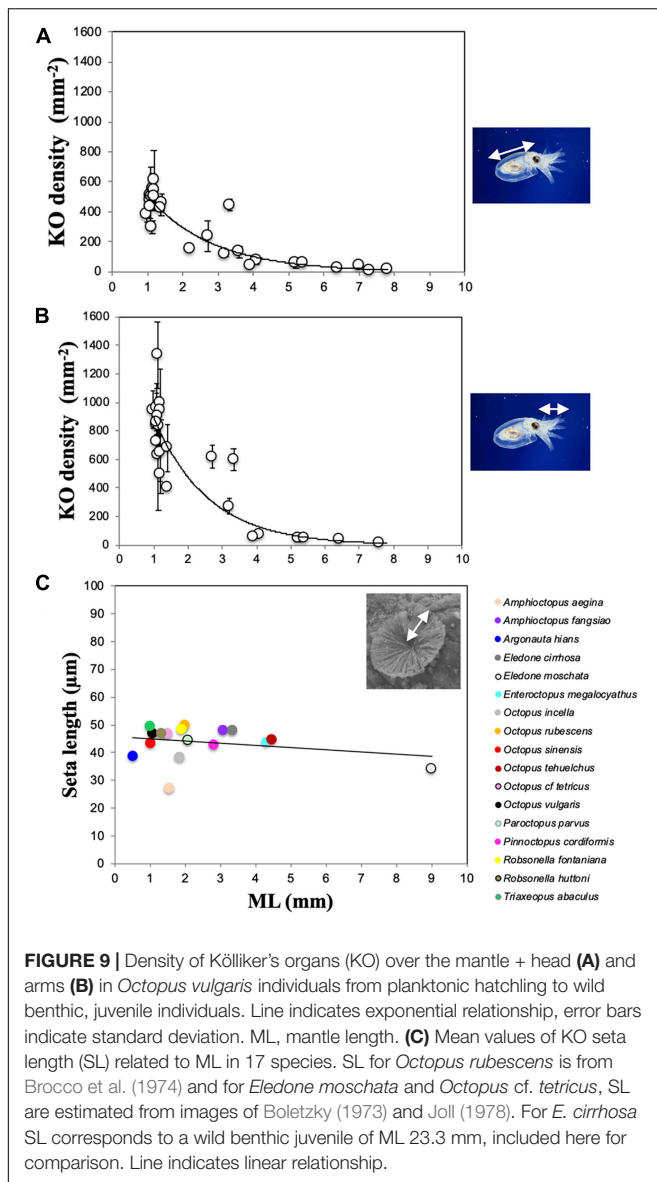
behavior that cause the eruption of the tufts and eversion and splaying of the setae on the epidermis is unknown. The basal muscles associated with the KO tuft suggest that tufts may be actively flexed or rotated (Brocco et al., 1974). Contraction of these basal muscles has been proposed to erupt the tuft and cause posterior eversion of the setae (Boletzky, 1978-1979; see his Figure 14). In the chaetae of groups such as the annelids, the muscles attached to the basal matrix of the chaetal sac are responsible for the movement of a single, a few, or the whole group of chaetae (Hausen, 2005). A similar process could be expected for the octopus KO. However, as far as we know, the setae (or chaetae) of other animal groups do not have the capacity to splay and radiate into the everted form observed in the octopus KO, with the possible exception of the long chaetae of trochophore larvae from sabellariid polychaetes (Pennington and Chia, 1984).

## Size and Density Patterns of KO Among Octopus Species

The size of the KO examined is fairly constant and, with the exception of *A. aegina*, SL ranges between 40 and 50  $\mu\text{m}$ , independent of the animal size. For example, the large hatchlings of *O. tehuelchus* (180 mg; Braga et al., 2021) are 130-fold heavier than those of *O. vulgaris* (1.4 mg; Villanueva, 1995) but the SL of both species is the same (Table 3). In addition, KO size seems not to change during ontogeny, at least in the only species surveyed through early growth, *O. vulgaris*. In this species, the uniform seta length, even in KO that appeared after hatching, indicates that KO size is independent of the exponential body growth of the young octopus, from planktonic hatchling to benthic juvenile, despite a weight increase of nearly 125 times (Villanueva, 1995).

Differential shrinkage can be expected between the skin and the KO due to fixation, preservation and microscopic treatments, including dehydration, as skin tissue contains more water than do the chitinous KO setae (Supplementary Table 1). Therefore, living animals probably have KO densities slightly lower than those recorded from the SEM images in the present study. This shrinkage may suggest that KO do not touch each other in live organisms, although touching was observed in some SEM images (see Figures 3F–H, 4G,H). Observations of live or fresh tissue will help to address this issue. Study of the elemental composition of the KO found sulphur to be the main component. High sulphur concentrations have been reported also in other hard structures of cephalopods, including the chitinous beaks (Hunt and Nixon, 1981), vestigial shell of octopus (Napoleao et al., 2005), squid gladius (Ichihashi et al., 2001) and the egg shell of cirrate octopods (Villanueva, 1992).

KO were observed covering the aboral surface of the arms of the octopuses examined but are absent from the oral side of both the arms and the interbrachial web, with the only exception of *A. aegina*, where KO were observed on both the oral and aboral arm tip (Figures 3E–H). In the species analyzed, the KO density over the arms seems to be equal or higher than that on mantle and head, giving a special relevance to the arms (Table 3 and Figures 8C,D). This density in KO on the arms decreases with increasing hatchling ML, remaining independent of ML for the mantle and head (Figures 8A,B). With the exception of two species with large hatchlings (*E. megalocyathus* and *O. tehuelchus*), the density of KO seems to be similar on the ventral and dorsal surfaces of the octopus species analyzed (Table 3). Therefore, the general trend corresponds to a hatchling octopus maintaining an almost equal density of KO over its ventral and dorsal surfaces; they tend to reach



higher densities on the aboral surface of the arms, but this tendency decreases with increasing size at hatching (species-specific characteristic) (Figure 8).

Observations of the arms of *O. vulgaris* confirms that new KO are added after hatching (Figure 10): new KO are generated even in specimens at the 52-sucker stage, indicating that KO are continuously added even after settlement, which usually happens when the animals have 30 suckers per arm at 2 months of life under culture conditions and rearing temperature of 21°C (Villanueva, 1995). In contrast, using SEM it was not possible to discern the existence of new KO added to the mantle after hatching, because of the difficulty of distinguishing hatching from post-hatching tissues anywhere other than toward the tip of each arm. In other large tegumental organs of early stages of octopuses, notably the chromatophores (Packard, 1988), specific arrangement patterns on the ventral and dorsal surfaces are

considered to be key taxonomic characters (Hochberg et al., 1992). In a similar way, the distribution of higher or lower KO densities over the mantle may help to discriminate among morphologically resembling octopod species sampled from the same geographic area. For example, *O. sinensis* and *T. abaculus*, both distributed in NW Pacific, are similar in size at hatching but they have very different KO densities: low numbers on *T. abaculus* but high on *O. sinensis* (Figure 8). The density of KO on *O. vulgaris* decreased with growth, probably due to limited addition of new KO, but also due to the notable increase of the overall surface area of the body. Therefore, species and age seem to be important factors determining KO densities. For example, the KO density in *O. vulgaris* decreased to low levels after the first month of life and to very low levels by 60 days when the animals become benthic, reaching a body size similar to the hatchlings of the holobenthic *O. tehuelchus* or the meropelagic *E. megalocyathus*, both of these latter species which, in contrast, at this size, are still fully covered by high densities of KO (see Table 3). The apparent degradation of KO was observed in the dorsal mantle of benthic juveniles of *O. vulgaris*, being characterized by the loss of setae and exposure of the basal KO musculature as a circular muscle stump. These muscle stumps on the skin surface were mingled with apparently functional KO, and may suggest that degradation would be a gradual process. It may be therefore possible to identify KO muscle stumps in the skin of subadult/adult individuals by the presence of small, circular muscle scars of around 27 μm in diameter.

## Possible KO Functions and an Evolutionary Perspective

As far as we know from microscopical and histochemical studies, no nervous tissue has been reported in connection with KO (Boletzky, 1973; Brocco et al., 1974; Accogli et al., 2017; González-Costa et al., 2020), excluding the suspected existence of neurons associated with the obliquely striated dermal muscle fibers of the organ. This may exclude a sensorial mechano- and/or chemoreceptor function for these organs. In addition, the absence of KO from the oral side of arms and suckers seems also to exclude a possible role in prey detection. Querner (1927) demonstrated with the Schultz reaction that KO tufts contain chitin and, recently, Accogli et al. (2017) and González-Costa et al. (2020) found positive staining for lectins in the KO setae, suggesting the presence of the proteoglycan N-acetylglucosamine, which would presumably have a mainly structural role because N-acetylglucosamine is a precursor for chitin synthesis. The same authors using histochemical techniques suggested that the absence of KO staining with periodic acid-Schiff (PAS) means that no secretory function can be attributed to this organ. It has been proposed that the relatively hard structure of the chitinous KO may assist hatching, preventing the animal slipping back into the chorion (Boletzky, 1978-1979). However, the presence of KO on the arms (which are not used to aid hatching), suggests that their function during hatching would be a secondary adaptation (Boletzky, 1992).

Naef (1923) suggested that KO may help in buoyancy. In this context, the present estimations showed that fully everted KO

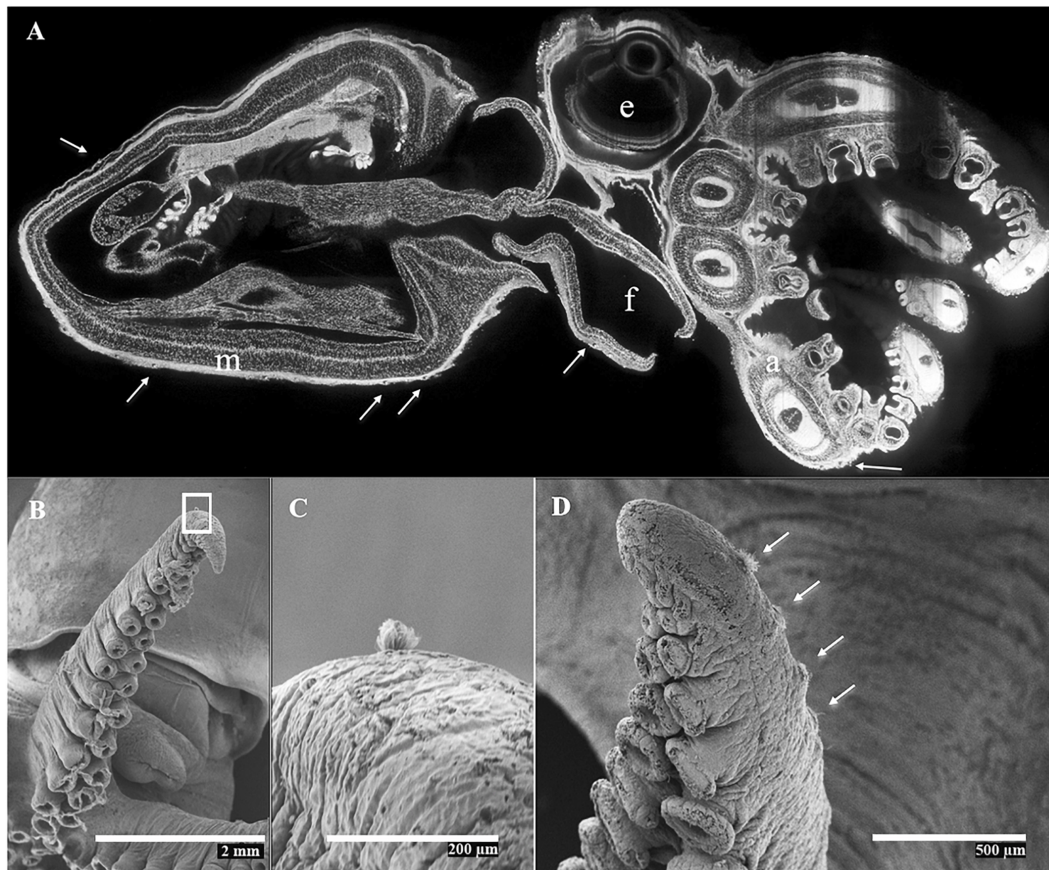


**FIGURE 10** | *Octopus vulgaris*. **(A)** Mid-sagittal SPIM image from a cultured individual aged 50 days, ML 5.8 mm, labeled with Evans blue and excited at 638 nm. Note the few Kölliker's organs (KO; white arrows) present on skin of mantle (m), funnel (f), and arms (a); e, (eye). **(B–D)** SEM images showing generation of new KO during the early benthic stage. **(B)** left arm III, with  $n = 30$  suckers from a cultured, recently benthic individual ML 9.3 mm (measured fresh), age 60 days, showing a KO near arm tip. **(C)** Magnified image of rectangle in **(B)**, showing semi-everted KO; **(D)**, right arm III, with  $n = 52$  suckers, from a wild benthic individual, ML 8.4 mm ML, showing KO (white arrows) near arm tip.

notably increased the body surface of the young octopus by a mean of 2/3 of the skin surface in comparison with skin areas with retracted KO. This modular body surface extension and accompanying rough texture probably influence flow forces (such as those of drag and propulsion) on the young octopus during specific times or stages of paralarval life, enhancing or restricting passive transport within oceanic currents and saving energy in a similar way as observed in other invertebrate larvae (Emlet, 1991; Ditsche and Summers, 2014; Waringer et al., 2020). Planktonic octopus hatchlings are quite similar to squid hatchlings in size and locomotion mode, both have a rounded mantle of a few mm in length and relatively large funnel apertures to use constantly during jet propulsion in the water column (Villanueva et al., 1997, 2016; Dan et al., 2020). Squid hatchlings operate at low and intermediate Reynolds numbers of  $1-10^2$  where inertia and viscosity have similar relative effects on flow (Thompson and Kier, 2002; Bartol et al., 2008, 2009; York et al., 2020). Here we assume low and intermediate Reynolds numbers also for planktonic octopus hatchlings which will permit some KO influence to increase drag and reduce sinking rate.

Considering other possible functions, Brocco et al. (1974) showed that KO tufts are strongly anisotropic and positively birefringent with respect to their long axis, changing from blue to yellow against a red background (Figure 1). We suggest that this character may support a possible function of KO related to body-outline disruption and camouflage. Young planktonic octopuses live in the water column, a luminous environment during the daytime, where birefringent skin surfaces may help the octopus against prey and predators, as does disruption of the body outline in adults by raising papillae in the skin (Mathger et al., 2009; Hanlon and Messenger, 2018). Diurnal descent dispersion has been observed for planktonic octopus under experimental conditions (Dan et al., 2020, 2021), a behavior which may benefit from both possible functions of the KO: drag generated by the everted setae may improve passive buoyancy; and their birefringent properties during daytime may be of help for camouflage. The absence of KO in deep-sea octopuses, far from the photic zone, may support this possible function of KO related with camouflage.

**TABLE 4 |** Mean seta length (SL), everted Kölliker's organ volume (EKOV), everted Kölliker's organ surface (EKOS), and resulting increased body surface (in percentage, %) when Kölliker's organs (KO) are fully everted compared with completely retracted.

Species	N	Age (d)	Mean seta length ( $\mu\text{m}$ )	EKOV ( $\mu\text{m}^3$ )	EKOS ( $\mu\text{m}^2$ )	Increased body surface when everted KO			
						Mantle + head (%)	Arms (%)	Ventral Surface (%)	Dorsal surface (%)
<i>Amphioctopus aegina</i>	7	0–7	27.5	43408	4741	61	67	64	63
<i>Amphioctopus fangsiao</i>	6	5–7	48.1	233000	14534	59	51		55
<i>Argonauta hians</i>	3	0	38.8	122018	9443	57	59	65	45
<i>Enteroctopus megalocyathus</i>	3	0	43.7	174571	11989	50	51	46	52
<i>Octopus sinensis</i>	6	12	43.5	171917	11868	81	86	84	84
<i>O. sinensis</i>	5	18	43.5 <sup>#</sup>	171917	11868	65	65	71	65
<i>Octopus tehuelchus</i>	3	0	44.6	185179	12470	79	76	35	81
<i>Octopus vulgaris</i>	13	0	46.9*	216056	13821	77	85	82	81
<i>O. vulgaris</i>	1	5	46.6	215083	13644	77	77	77	
<i>O. vulgaris</i>	1	10	46.9*	216056	13821	75	73		
<i>O. vulgaris</i>	3	19	46.9*	216056	13821	62	81	62	71
<i>O. vulgaris</i>	2	30	46.9*	216056	13821	47	65	48	54
<i>O. vulgaris</i>	1	42	47.5	224334	14176	35	34	40	33
<i>O. vulgaris</i>	1	46	46.9*	216056	13821	22	28		25
<i>O. vulgaris</i>	3	50	47.6	211477	14236	29	25	31	26
<i>O. vulgaris</i>	2	60	46.9*	216056	13821	19	21	20	8
<i>O. vulgaris</i>	4	?	46.7	185179	13703	8	10	8	9
<i>Pinnoctopus cordiformis</i>	6	0	43.0	166515	11618	43	79	78	67
<i>Robsonella fontaniana</i>	3	0	48.5	238194	14780	56	87	76	72
<i>Robsonella huttoni</i>	6	0	46.9	216056	13821	41	84	80	76
<i>Tritaxoopus abaculus</i>	6	0	49.5	254018	15395	65	78	72	67

To estimate the body surface increase, the KO density from Mantle + head and Arms body areas as well as from ventral and dorsal surface of the animal, were used. N, number of individuals examined; d, age in days. (<sup>#</sup>) For *Octopus sinensis* aged 18 days, no everted KO were observed and in consequence SL was not obtained; for this age, the mean SL obtained for individuals aged 12 days was used. (\*) For *O. vulgaris* aged 0, 19, 30, 46, and 60 days no everted KO were observed and SL was not obtained. As no significant differences were observed within SL of other ages in this species, the mean value of 46.9  $\mu\text{m}$  for SL was assumed as an estimation for these ages. Individuals marked with unknown age (?) correspond to wild benthic specimens of four *O. vulgaris* 7.3–8.3 mm ML.

The presence of KO on the juveniles of holobenthic species such as *A. fangsiao*, *E. moschata* and *O. tehuelchus*, does not seem to fit hypotheses associated with camouflage or drag force hypotheses. However, KO may represent a plesiomorphic feature retained from their ancestors. In this way, KO are present in hatchlings of all modes of incirrate octopod life cycles: holopelagic, holobenthic and meropelagic, and no trace of KO has been found on embryos of cirrate octopods (Boletzky, 1982).

To date, all examined meropelagic octopuses possess KO, which are absent only from large, holobenthic hatchlings of incirrate species (*G. pacifica*, *O. briareus*, and *O. maya*). This seems to be more consistent with the hypothesis of the radiation of octopuses by evolution from a meropelagic ancestor characterized by small to medium-sized hatchlings and planktonic early life (Ibáñez et al., 2018). Assuming KO are associated with the planktonic phase, their presence in some holobenthic species indicated above (*A. fangsiao*, *E. moschata*, *Octopus* cf. *joubini* and *O. tehuelchus*) may suggest that these are examples of intermediate apomorphic characters in incirrate octopod taxa that reached the holobenthic mode of life more recently.

Chun (1915) indicated that in the holopelagic octopod *Bolitaena pygmaea*, KO persist over a long period, without

specifying animal size. The presence/absence and degree of development of KO in subadult and adult holopelagic octopods merits further research and their presence may be interpreted as support for the neotenus origin of the holopelagic octopods, as suggested by Strugnell et al. (2004). Conversely, the KO may be adaptive for the reasons we identify here.

In addition to the KO studied here, an intriguing Kölliker's organ-like structure was described by Hoyle (1904) from *Octopus arborescens*, a tiny species (mature at a ML of around 10 mm; IGG, unpublished) collected from littoral waters of Sri Lanka, the Seychelles and off Zanzibar (Hoyle, 1907). The species was named for the presence of arborescent skin papillae. The illustrations of the distribution and histological sections of these organs, located at the distal end of the skin papillae, describing "radiating fibres" of 60  $\mu\text{m}$  length (Hoyle, 1904, Plate III, **Figures 9–11**), match the general morphology and setae length of everted KO. The relationship of these organs with the KO described here is unclear, especially since they are described from adult (although tiny) specimens. Adam (1939) described and illustrated similar structures in *Octopus* sp. larvae collected in surface waters near Saint Peter and Paul Rocks, central Atlantic, and considered them as a large, second type of KO equivalent to those described by Hoyle (1904).

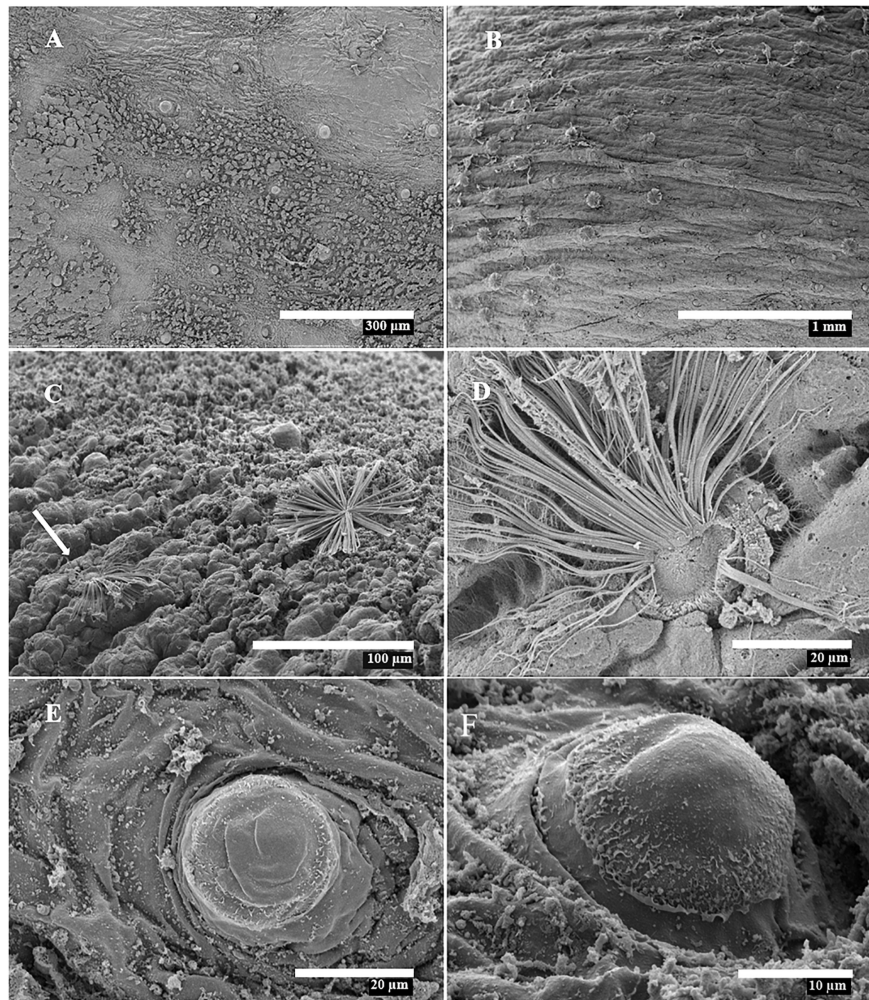


**FIGURE 11** | Scanning Electron Microscopy images of wild-caught *Octopus vulgaris* showing Kölliker's organ (KO) degradation. **(A,B)** ML 8.6 mm, dorsal mantle surface; **(C–F)** ML 8.1 mm, dorsal mantle and arm. **(A)** KO muscle stumps distributed on skin. **(B)** Muscle stumps together with apparently functional KO. **(C)** Degraded (white arrow) and functional KO on left arm I. **(D)** Detail of degraded KO from **(C)**. **(E,F)** Muscle stumps of degraded KO on mantle.

## CONCLUSION

The KO surveyed in the present study are organs of consistent structure with a taxonomic and body distribution unrelated to hatchling size but reaching higher densities on the arms in most species. The organ is also consistent in size and structure through ontogeny (at least in *O. vulgaris*, the only species for which an ontogenetic series was available). The modular eversion of KO increases skin roughness and, notably, the body surface area by an approximate extra 2/3, probably influencing flow forces such as drag. The birefringent properties and relatively hard structure of the setae from the KO that spread over the skin of planktonic octopuses have a number of different possible functions. Camouflage and the saving of locomotion energy may be complementary functions working together during daytime when planktonic octopuses descend in the water column. Future observations on living animals will be necessary to investigate these hypotheses as well as the possible interactions between

KO and the mucus layer covering the skin surface of the individuals. Whether or not the presence of KO in some species with direct benthic hatchlings is a redundant plesiomorphic character, indicative of a recent meropelagic origin, also requires further investigation.

## AUTHOR'S NOTE

This work is dedicated to the memory of Sigurd von Boletzky, who passed away on September 28, 2020.

## DATA AVAILABILITY STATEMENT

The original contributions presented in the study are included in the article/**Supplementary Material**, further inquiries can be directed to the corresponding author/s.

## ETHICS STATEMENT

The animal study was reviewed and approved by the authors, who declare that the national laws regarding the care and welfare of laboratory animals were followed. Hatchlings of *Octopus vulgaris* were obtained under the project “Practice of handling, behavior, haemolymph extraction and euthanasia in cephalopods: *Sepia officinalis* (cuttlefish) and *O. vulgaris* (octopus)” Ref. 10243, approved by the ICM ethics committee and the local government, in accordance with the requirements imposed by the Directive 2010/63/EU on the protection of animals used for scientific purposes. Embryos and hatchlings of *O. maya* were prepared following the directive approved by the Animal Ethics Committee of the Faculty of Chemistry at Universidad Nacional Autónoma de México (UNAM, Sisal). Permit Number: Oficio/FQ/CICUAL/099/15.

## AUTHOR CONTRIBUTIONS

RV conceived and designed the study, contributed specimens, recorded most SEM images, performed the data analysis and wrote the first draft. MC-L and JS prepared samples for SPIM imaging and recorded and analyzed SPIM images. JN contributed specimens and recorded SEM images. OE and FF-Á contributed specimens and provided laboratory support. SC, IGG, NO, CR, and JV contributed with specimens. LB-P and PS provided laboratory support and analysis. All authors helped prepare and revise the manuscript, interpreted the findings together, and approved the final version of the manuscript.

## FUNDING

FF-Á was supported by an Irish Research Council–Government of Ireland Postdoctoral Fellowship Award (Ref. GOIPD/2019/460). Material contributed by IGG was collected partly through the support of funding from the Japan Science and Technology Agency (grant nos. J130000263, J170000574, AS2715164U and AS0138002); and partly through travel support from the Okinawa Institute of Science and Technology (OIST). SC acknowledges

## REFERENCES

- Accogli, G., Scillitani, G., Mentino, D., and Desantis, S. (2017). Characterization of the skin mucus in the common octopus *Octopus vulgaris* (Cuvier) reared paralarvae. *Eur. J. Histochem.* 61, 2815.
- Adam, W. (1939). A propos des organes épithéliaux (Köllikersche Büschel) chez une larve d'Octopode. *Mém. Mus. R. Hist. Nat. Belg.* 15, 123–134.
- Alejo-Plata, M., and Herrera-Alejo, S. (2014). First description of eggs and paralarvae of green octopus *Octopus hubbsorum* (Cephalopoda: Octopodidae) under laboratory conditions. *Am. Malacol. Bull.* 32, 132–139. doi: 10.4003/006.032.0101
- Bartol, I. K., Krueger, P. S., Stewart, W. J., and Thompson, J. T. (2009). Pulsed jet dynamics of squid hatchlings at intermediate Reynolds numbers. *J. Exp. Biol.* 212, 1506–1518. doi: 10.1242/jeb.026948
- Bartol, I. K., Krueger, P. S., Thompson, J. T., and Stewart, W. J. (2008). Swimming dynamics and propulsive efficiency of squids throughout ontogeny. *Integr. Comp. Biol.* 48, 720–733. doi: 10.1093/icb/icn043

the funding of a FONDECYT research grant (#11170617). Part of material contributed by NO was obtained under the project PICT 201 0670 from the National Agency for Scientific and Technological Research of Argentina. Project funding and support to RV was provided by the Spanish Ministry of Science, Innovation and Universities (OCTOSET project, RTI2018-097908-B-I00, MCIU/AEI/FEDER, EU), the Spanish Ministry of Education (grant PRX19/00153) and the Spanish government through the “Severo Ochoa Center of Excellence” accreditation (CEX2019-000928-S).

## ACKNOWLEDGMENTS

RV is very grateful to the valuable help and expertise of Mr. Jose Manuel Fortuño (Institut de Ciències del Mar, Barcelona) and Mrs. Géraldine Toutirais (Muséum National d'Histoire Naturelle, Paris), responsible for the SEM services where many images were obtained. IGG is most grateful to Jonathan Miller and his group at OIST for obtaining and raising the octopuses from which some of the hatchlings were obtained, and for their help and support with associated experiments carried out by IGG at the OIST labs. IGG also thanks Leo Che and Moemi Kanno for their technical help with raising and maintaining octopuses at Tohoku University Graduate School of Science, including hatchlings of *O. sinensis*, *A. fangsiao*, and '*O.*' *parvus*. Specimens of *A. fangsiao* were collected from Futtsu, Tokyo Bay, with the help of Leo Che, Germaine Lau, and Delta Putra; and of '*O.*' *parvus* from Amakusa, with the help of Mr. Yukimi (Amakusa, Kyushu) and Hiroki Takahashi and Hiroto Teranaka (Kami-Amakusa City Hall, Kumamoto, Kyushu). We thank M. Heyward Boyette, Jr., DVM and Dr. Nicolás Battini, for the photographs depicted in **Figure 1**. Comments from the associate editor and four reviewers greatly improved the final version.

## SUPPLEMENTARY MATERIAL

The Supplementary Material for this article can be found online at: <https://www.frontiersin.org/articles/10.3389/fmars.2021.645738/full#supplementary-material>

- Batham, E. J. (1957). Care of eggs by *Octopus maorum*. *Trans. R. Soc. N. Z.* 84, 629–638.
- Boletzky, S. V. (1969). Zum Vergleich der Ontogenesen von *Octopus vulgaris*, *O. joubini* und *O. briareus*. *Rev. Suisse Zool.* 76, 716–726.
- Boletzky, S. V. (1973). Structure and function of the Kölliker organs in young octopods (Mollusca, Cephalopoda). *Z. Morphol. Tiere* 75, 315–327. doi: 10.1007/bf00288477
- Boletzky, S. V. (1977). Post-hatching behavior and mode of life in cephalopods. *Symp. Zool. Soc. Lond.* 38, 557–567.
- Boletzky, S. V. (1982). On eggs and embryos of cirromorph octopods. *Malacologia* 22, 197–204.
- Boletzky, S. V. (1984). The embryonic development of the octopus *Scaeuargus unicirrhus* (Mollusca, Cephalopoda). Additional data and discussion. *Vie Milieu* 334, 87–93.
- Boletzky, S. V. (1992). Evolutionary aspects of development, life style, and reproductive mode in incirrate octopods (Mollusca, Cephalopoda). *Rev. Suisse Zool.* 99, 755–770. doi: 10.5962/bhl.part.79852

- Boletzky, S. V., Fuentès, M., and Offner, N. (2002). Development features of *Octopus macropus* Risso, 1826 (Mollusca, Cephalopoda). *Vie Milieu* 52, 209–215.
- Boletzky, S. V., Fuentès, M., and Offner, N. (2001). First record of spawning and embryonic development in *Octopus macropus* (Mollusca: Cephalopoda). *J. Mar. Biol. Assoc. U.K.* 81, 703–704.
- Boletzky, S. V. (1978–1979). Nos connaissances actuelles sur le développement des octopodes. *Vie Milieu* 28–29, 85–120.
- Braga, R., Van der Molen, S., Pontones, J., and Ortiz, N. (2021). Embryonic development, hatching time and newborn juveniles of *Octopus tehuelchus* under two culture temperatures. *Aquaculture* 530:735778. doi: 10.1016/j.aquaculture.2020.735778
- Brocco, S. L., O'Clair, R., and Cloney, R. A. (1974). Cephalopod integument: the ultrastructure of Kölliker's organs and their relationship to setae. *Cell Tissue Res.* 151, 293–308.
- Budelmann, B., Schipp, R., and Boletzky, S. V. (1997). "Cephalopoda," in *Microscopic Anatomy of Invertebrates*, Vol. 6A, eds F. W. Harrison and A. J. Kohn (New York, NY: Wiley-Liss, Inc), 119–414.
- Carrasco, S. A. (2014). The early life history of two sympatric New Zealand octopuses: eggs and paralarvae of *Octopus huttoni* and *Pinnoctopus cordiformis*. *New Zeal. J. Zool.* 41, 32–45. doi: 10.1080/03014223.2013.827126
- Chun, C. (1915). "The Cephalopoda," in Part I: Oegopsida, Part II: Myopsida, Octopoda. Scientific Results of the German Deep-Sea Expeditions on Board the Steamship "Valdivia" 1898–1899, Vol. 18 (Jerusalem: Israel Program for Scientific Translations).
- Cyran, N., Staedler, Y., Schönenberger, J., Klepal, W., and von Byern, J. (2013). Hatching glands in cephalopods - A comparative study. *Zool. Anz.* 253, 66–82. doi: 10.1016/j.jcz.2013.04.001
- Dan, S., Shibasaki, S., Takasugi, A., Takeshima, S., Yamazaki, H., Ito, A., et al. (2021). Changes in behavioural patterns from swimming to clinging, shelter utilization and prey preference of East Asian common octopus *Octopus sinensis* during the settlement process under laboratory conditions. *J. Exp. Mar. Biol. Ecol.* 539, 151537. doi: 10.1016/j.jembe.2021.151537
- Dan, S., Takasugi, A., Shibasaki, S., Oka, M., and Hamasaki, K. (2020). Ontogenic change in the vertical swimming of East Asian common octopus *Octopus sinensis* paralarvae under different water flow conditions. *Aquat. Ecol.* 54, 795–812. doi: 10.1007/s10452-020-09777-7
- Ditsche, P., and Summers, A. P. (2014). Aquatic versus terrestrial attachment: water makes a difference. *Beilstein J. Nanotechnol.* 5, 2424–2439. doi: 10.3762/bjnano.5.252
- Emler, R. B. (1991). Functional constraints on the evolution of larval forms of marine invertebrates: experimental and comparative evidence. *Am. Zool.* 31, 707–725. doi: 10.1093/icb/31.4.707
- Felgenhauer, B. E. (1987). Techniques for preparing crustaceans for scanning electron microscopy. *J. Crustac. Biol.* 7, 71–76. doi: 10.1163/193724087x00054
- Fiorito, G., Affuso, A., Basil, J., Cole, A., de Girolamo, P., D'Angelo, L., et al. (2015). Guidelines for the Care and Welfare of Cephalopods in Research – A consensus based on an initiative by CephRes, FELASA and the Boyd Group. *Lab. Anim.* 49, 1–90. doi: 10.1177/0023677215580006
- Fioroni, P. (1962). Die embryonale Entwicklung der Köllikerschen Organe von *Octopus vulgaris* Lam. *Rev. Suisse Zool.* 69, 497–511. doi: 10.5962/bhl.part.75586
- González-Costa, A., Fernández-Gago, R., Carid, S., and Molist, P. (2020). Characterisation in the *Octopus vulgaris* skin throughout its life cycle. *Anat. Histol. Embryol.* 49, 502–510. doi: 10.1111/ah.12554
- Gordon, D. P. (1975). The resemblance of bryozoan gizzard teeth to "annelid-like" setae. *Acta Zool.* 56, 283–289. doi: 10.1111/j.1463-6395.1975.tb00105.x
- Gustus, R. M., and Cloney, R. A. (1972). Ultrastructural similarities between setae of Brachiopods and Polychaetes. *Acta Zool.* 53, 229–233. doi: 10.1111/j.1463-6395.1972.tb00590.x
- Gustus, R. M., and Cloney, R. A. (1973). Ultrastructure of the larval compound setae of the polychaete *Nereis vexillosa* Grube. *J. Morphol.* 140, 355–366. doi: 10.1002/jmor.1051400308
- Hanlon, R. T., and Messenger, J. B. (2018). *Cephalopod Behaviour*, 2nd Edn. Cambridge: Cambridge University Press. doi: 10.1017/9780511843600
- Hausen, H. (2005). Chaetae and chaetogenesis in polychaetes (Annelida). *Hydrobiologia* 535, 37–52. doi: 10.1007/s10750-004-1836-8
- Hochberg, F. G., Nixon, M., and Toll, R. B. (1992). "Order Octopoda Leach, 1818," in *Larval and Juvenile Cephalopods: A Manual for their Identification*, eds M. J. Sweeney, C. F. E. Roper, K. M. Mangold, M. R. Clarke, and S. V. Boletzky (Washington, DC: Smithsonian Institution Press), 213–280.
- Hoyle, W. E. (1904). Report on the Cephalopoda Collected by Professor Herdman, at Ceylon, in 1902. *Rep. Gov. Ceylon Pearl Oyster Fish.* 14, 185–200.
- Hoyle, W. E. (1907). The Marine Fauna of Zanzibar and East Africa, from collections made by Cyril Crowland in 1901–1902. The Cephalopoda. *Proc. Zool. Soc. Lond.* 77, 128–137.
- Huffard, C. L., Gentry, B. A., and Gentry, D. W. (2009). Description of the paralarvae of *Wunderpus photogenicus* Hochberg, Norman & Finn, 2006 (Cephalopoda: Octopodidae). *Raffles Bull. Zool.* 57, 109–112.
- Hunt, S., and Nixon, M. (1981). A comparative study of protein composition in the chitin-protein complexes of the beak, pen, sucker disc, radula and oesophageal cuticle of cephalopods. *Comp. Biochem. Physiol. Part B Biochem.* 68, 535–546. doi: 10.1016/0305-0491(81)90071-7
- Ibáñez, C. M., Rezende, E. L., Sepúlveda, R. D., Avaria-Llatureo, J., Hernández, C. E., Sellanes, J., et al. (2018). Thorson's rule, life-history evolution, and diversification of benthic octopuses (Cephalopoda: Octopodoidea). *Evolution* 72, 1829–1839. doi: 10.1111/evo.13559
- Ichihashi, H., Kohno, H., Kannan, K., Tsumura, A., and Yamasaki, S.-I. (2001). Multielemental analysis of purpleback flying squid using high resolution inductively coupled plasma-mass spectrometry (HR ICP-MS). *Environ. Sci. Technol.* 35, 3103–3108. doi: 10.1021/es010653v
- Jerreb, P., Roper, C. F. E., Norman, M. D., and Finn, J. K. (2013). *Cephalopods of the World. An Annotated and Illustrated Catalogue of Cephalopod Species Known to Date. Volume 3. Octopods and Vampire Squids. FAO Species Catalogue for Fishery Purposes.* (Rome: FAO), 370.
- Joll, L. M. (1978). Observations on the embryonic development of *Octopus tetricus* (Mollusca: Cephalopoda). *Aust. J. Mar. Freshw. Res.* 29, 19–30. doi: 10.1071/mf9780019
- Kölliker, A. (1844). *Entwicklungsgeschichte der Cephalopoden*. Zürich: Meyer und Zeller.
- Leise, E. M., and Cloney, R. A. (1982). Chiton integument: ultrastructure of the sensory hairs of *Mopalia muscosa* (Mollusca: Polyplacophora). *Cell Tissue Res.* 223, 43–59. doi: 10.1007/bf00221498
- Lincoln, R., Boxshall, G., and Clarke, P. (1998). *A Dictionary of Ecology, Evolution and Systematics*, 2nd Edn. Cambridge: Cambridge University Press.
- Lüter, C. (2000). Ultrastructure of larval and adult setae of Brachiopoda. *Zool. Anz.* 239, 75–90.
- Maldonado, E., Rangel-Huerta, E., González-Gómez, R., Fajardo-Alvarado, G., and Morillo-Velarde, P. S. (2019). *Octopus insularis* as a new marine model for evolutionary developmental biology. *Biol. Open* 8:bio046086. doi: 10.1242/bio.046086
- Mangold, K., Boletzky, S. V., and Frösch, D. (1971). Reproductive biology and embryonic development of *Eledone cirrhosa* (Cephalopoda, Octopoda). *Mar. Biol.* 8, 109–117. doi: 10.1007/bf00350926
- Mangold (1922–2003), K., Vecchione, M., and Young, R. E. (2018). *Tremoctopodidae Tryon, 1879. Tremoctopus Chiaie 1830. Blanket octopus. Version 29 March 2018.* Available online at: <http://tolweb.org/Tremoctopus/20202/2018.03.29>
- Mangold-Wirz, K., Boletzky, S. V., and Mesnil, B. (1976). Biologie de reproduction et distribution d'*Octopus salutti* Verany (Cephalopoda, Octopoda). *Rapp. Comm. Int. pour l'Explor. Sci. Méditerr.* 23, 83–97.
- Mathger, L. M., Shashar, N., and Hanlon, R. T. (2009). Do cephalopods communicate using polarized light reflections from their skin? *J. Exp. Biol.* 212, 2133–2140. doi: 10.1242/jeb.020800
- Merz, R. A., and Woodin, S. A. (2006). Polychaete chaetae: Function, fossils, and phylogeny. *Integr. Comp. Biol.* 46, 481–496. doi: 10.1093/icb/ijc057
- Naef, A. (1923). "Die Cephalopoden," in *Fauna e Flora del Golfo di Napoli. Monographie 35, Vol. I, Parts I and II, Sistematik*, ed. A. Mercado (Jerusalem: Israel Program for Scientific Translations), 1–863. doi: 10.1007/bf02955569
- Naef, A. (1928). *Cephalopoda, Embryology. Part I, Vol II (Final part of Monograph No. 35)*. Washington, DC: Smithsonian Institution Libraries.
- Napoleao, P., Sousa-Reis, C., Alves, L. C., and Pinheiro, T. (2005). Morphologic characterisation and elemental distribution of *Octopus vulgaris* Cuvier, 1797

- vestigial shell. *Nucl. Inst. Methods Phys. Res. Sect. B Beam Interact. Mater. Atoms.* 231, 345–349. doi: 10.1016/j.nimb.2005.01.081
- Nesis, K. N. (1979). Larvae of cephalopods. *Biologiya Morya*, 4, 26–37. [In Russian, English translation 1980. *Soviet J. Mar. Biol.* 5, 267–275.]
- Nödl, M. T., Fossati, S. M., Domingues, P., Sanchez, F. J., and Zullo, L. (2015). The making of an octopus arm. *Evodevo* 6:19. doi: 10.1186/s13227-015-0012-8
- Ortiz, N., Ré, M. A., and Márquez, F. (2006). First description of eggs, hatchlings and hatchling behaviour of *Enteroctopus megalocyathus* (Cephalopoda: Octopodidae). *J. Plankton Res.* 28, 881–890. doi: 10.1093/plankt/fbl023
- Ortiz, N., and Ré, M. E. (2011). The eggs and hatchlings of the octopus *Robsonella fontaniana* (Cephalopoda: Octopodidae). *J. Mar. Biol. Assoc. U.K.* 9, 705–713. doi: 10.1017/s0025315410001232
- Overath, H., and Boletzky, S. V. (1974). Laboratory observations on spawning and embryonic development of a blue-ringed octopus. *Mar. Biol.* 27, 333–337. doi: 10.1007/bf00394369
- Packard, A. (1988). “The skin of the Cephalopods (coleoids): general and special adaptations,” in *The Mollusca. Volume 11. Form and Function*, eds E. R. Trueman, and M. R. Clarke (San Diego, CA: Academic Press), 37–67. doi: 10.1016/b978-0-12-751411-6.50010-2
- Pennington, J. T., and Chia, F.-S. (1984). Morphological and behavioral defenses of Trochophore larvae of *Sabellaria cementarium* (Polychaeta) against four planktonic predators. *Biol. Bull.* 167, 168–175. doi: 10.2307/1541345
- Promboon, P., Nabhitabhata, J., and Duengdee, T. (2011). Life cycle of the marbled octopus, *Amphioctopus aegina* (Gray) (Cephalopoda: Octopodidae) reared in the laboratory. *Sci. Mar.* 75, 811–821. doi: 10.3989/scimar.2011.75n4811
- Querner, F. V. (1927). Die Köllikerschen Büschel jugendlicher Octopoden, nebst einigen Bemerkungen zur Histologie der Haut dieser Formen. *Z. Zellforsch. Mikosk. Anat.* 4, 237–265. doi: 10.1007/bf01094554
- Quintana, L., and Sharpe, J. (2011). Preparation of mouse embryos for optical projection tomography imaging. *Cold Spring Harb. Protoc.* 2011:pdb.prot5639. doi: 10.1101/pdb.prot5639
- Schindelin, J., Arganda-Carreras, I., Frise, E., Kaynig, V., Longair, M., Pietzsch, T., et al. (2012). Fiji: an open-source platform for biological-image analysis. *Nat. Methods* 9, 676–682. doi: 10.1038/nmeth.2019
- Strugnell, J., Norman, M., Drummond, A. J., and Cooper, A. (2004). Neotenus origins for pelagic octopuses. *Curr. Biol.* 14, R300–R301. doi: 10.1016/j.cub.2004.03.048
- Sukhsangchan, C., and Nabhitabhata, J. (2007). Embryonic development of muddy paper nautilus, *Argonauta hians* Lightfoot, 1786, from Andaman Sea, Thailand. *Kasetsart J.* 41, 531–538.
- Swoger, J., Muzzopappa, M., López-Schier, H., and Sharpe, J. (2011). 4D retrospective lineage tracing using SPIM for zebrafish organogenesis studies. *J. Biophotonics* 4, 122–134. doi: 10.1002/jbio.201000087
- Thompson, J. T., and Kier, W. M. (2002). Ontogeny of squid mantle function: changes in the mechanics of escape-jet locomotion in the oval squid, *Sepioteuthis lessoniana* Lesson, 1830. *Biol. Bull.* 203, 14–26. doi: 10.2307/1543454
- Villanueva, R. (1992). Continuous spawning in the cirrate octopods *Opisthoteuthis agassizii* and *O. vossi*: features of sexual maturation defining a reproductive strategy in cephalopods. *Mar. Biol.* 114, 265–275. doi: 10.1007/BF00349529
- Villanueva, R. (1995). Experimental rearing and growth of planktonic *Octopus vulgaris* from hatching to settlement. *Can. J. Fish. Aquat. Sci.* 52, 2639–2650. doi: 10.1139/f95-853
- Villanueva, R., and Norman, M. D. (2008). Biology of the planktonic stages of benthic octopuses. *Oceanogr. Mar. Biol.* 46, 105–202. doi: 10.1201/9781420065756.ch4
- Villanueva, R., Nozais, C., and Boletzky, S. V. (1997). Swimming behaviour and food searching in planktonic *Octopus vulgaris* Cuvier from hatching to settlement. *J. Exp. Mar. Biol. Ecol.* 208, 169–184. doi: 10.1016/S0022-0981(96)02670-6
- Villanueva, R., Vidal, E. A. G., Fernández-Álvarez, F. Á., and Nabhitabhata, J. (2016). Early mode of life and hatchling size in cephalopod molluscs: influence on the species distributional ranges. *PLoS One* 11:e0165334. doi: 10.1371/journal.pone.0165334
- Voight, J. R., and Drazen, J. C. (2004). Hatchlings of the deep-sea octopus *Graledone boreopacifica* are the largest and most advanced known. *J. Molluscan Stud.* 70, 406–408.
- Waringer, J., Vitecek, S., Martini, J., Zित्रा, C., Handschuh, S., Vieira, A., et al. (2020). Hydraulic stress parameters of a cased caddis larva (*Drusus biguttatus*) using spatio-temporally filtered velocity measurements. *Hydrobiologia* 847, 3437–3451. doi: 10.1007/s10750-020-04349-0
- York, C. A., Bartol, I. K., Krueger, P. S., and Thompson, J. T. (2020). Squids use multiple escape jet patterns throughout ontogeny. *Biol. Open* 9:bio054585. doi: 10.1242/bio.054585
- Young, R. E., Harman, R. F., and Hochberg, F. G. (1989). Octopodid paralarvae from Hawaiian waters. *Veliger* 32, 152–165.

**Conflict of Interest:** The authors declare that the research was conducted in the absence of any commercial or financial relationships that could be construed as a potential conflict of interest.

*Citation:* Villanueva R, Coll-Lladó M, Bonnaud-Ponticelli L, Carrasco SA, Escolar O, Fernández-Álvarez FÁ, Gleadall IG, Nabhitabhata J, Ortiz N, Rosas C, Sánchez P, Voight JR and Swoger J (2021) Born With Bristles: New Insights on the Kölliker's Organs of Octopus Skin. *Front. Mar. Sci.* 8:645738. doi: 10.3389/fmars.2021.645738

Copyright © 2021 Villanueva, Coll-Lladó, Bonnaud-Ponticelli, Carrasco, Escolar, Fernández-Álvarez, Gleadall, Nabhitabhata, Ortiz, Rosas, Sánchez, Voight and Swoger. This is an open-access article distributed under the terms of the Creative Commons Attribution License (CC BY). The use, distribution or reproduction in other forums is permitted, provided the original author(s) and the copyright owner(s) are credited and that the original publication in this journal is cited, in accordance with accepted academic practice. No use, distribution or reproduction is permitted which does not comply with these terms.